

AD-A055 175

APPLIED DEVICES CORP KISSIMMEE FL  
A MODULAR ADAPTIVE, VARIABLE FUNCTION FLIGHT CONTROL SENSOR.(U)  
OCT 77 R PITTMAN

F/G 1/4

F33615-75-C-3154

UNCLASSIFIED

AFFDL-TR-77-112

NL

1 OF  
AD  
A055175



END  
DATE  
FILMED  
7-78  
DDC

AFFDL-TR-77-112

FOR FURTHER TRAN

② ✓

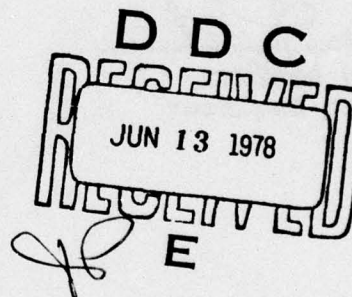
AD A 055175

# A MODULAR ADAPTIVE, VARIABLE FUNCTION FLIGHT CONTROL SENSOR

APPLIED DEVICES CORPORATION  
KISSIMMEE, FLORIDA

OCTOBER 1977

TECHNICAL REPORT AFFDL-TR-77-112  
Final Report for Period March 1975 - February 1977



Approved for public release; distribution unlimited.

78 06 12 155

AIR FORCE FLIGHT DYNAMICS LABORATORY  
AIR FORCE WRIGHT AERONAUTICAL LABORATORIES  
AIR FORCE SYSTEMS COMMAND  
WRIGHT-PATTERSON AIR FORCE BASE, OHIO 45433

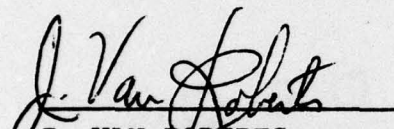
AU M7, UDC FILE COPY

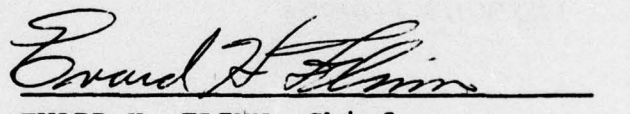
# NOTICE

When Government drawings, specifications, or other data are used for any purpose other than in connection with a definitely related Government procurement operation, the United States Government thereby incurs no responsibility nor any obligation whatsoever; and the fact that the Government may have formulated, furnished, or in any way supplied the said drawings, specifications, or other data, is not to be regarded by implication or otherwise as in any manner licensing the holder or any other person or corporation, or conveying any rights or permission to manufacture, use, or sell any patented invention that may in any way be related thereto.

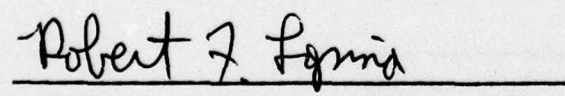
This report has been reviewed by the Information Office (IO) and is releasable to the National Technical Information Service (NTIS). At NTIS, it will be available to the general public, including foreign nations.

This technical report has been reviewed and is approved for publication.

  
J. VAN ROBERTS  
Project Engineer

  
EVARD H. FLINN, Chief  
Control Systems Development Branch  
Flight Control Division  
AF Flight Dynamics Laboratory

FOR THE COMMANDER

  
ROBERT F. LOPINA, Colonel, USAF  
Chief  
Flight Control Division  
AF Flight Dynamics Laboratory

Copies of this report should not be returned unless return is required by security considerations, contractual obligations, or notice on a specific document.



SECURITY CLASSIFICATION OF THIS PAGE (When Data Entered)

<p>1. REPORT NUMBER AFFDL/IR-77-112</p>		<p>2. GOVT ACCESSION NO.</p>		<p>3. RECIPIENT'S CATALOG NUMBER</p>	
<p>4. TITLE (and Subtitle) A MODULAR ADAPTIVE, VARIABLE FUNCTION FLIGHT CONTROL SENSOR.</p>				<p>5. TYPE OF REPORT &amp; PERIOD COVERED Final Research and Development Mar. '75 to Feb. '77</p>	
<p>6. AUTHOR(s) Roland/Pittman</p>				<p>7. CONTRACT OR GRANT NUMBER(s) F33(615)-75-C-3154</p>	
<p>8. PERFORMING ORGANIZATION NAME AND ADDRESS Applied Devices Corporation 2931 North Poinciana Boulevard Kissimmee, Florida 32741</p>				<p>9. AREA &amp; WORK CENTER PROJECT NAME Project 2403 Task: 02 Work Unit: 21</p>	
<p>10. CONTROLLING OFFICE NAME AND ADDRESS Air Force Flight Dynamics Laboratory Air Force Systems Command Wright-Patterson Air Force Base</p>				<p>11. REPORT DATE October 1977</p>	
<p>12. MONITORING AGENCY NAME &amp; ADDRESS (if different from Controlling Office) Final rept. Mar 75-Feb 77</p>				<p>13. SECURITY CLASS. (of this report) Unclassified</p>	
<p>14. DISTRIBUTION STATEMENT (of this Report) Approved for public release; distribution unlimited.</p>					
<p>15. DISTRIBUTION STATEMENT (of the abstract entered in Block 20, if different from Report)</p>					
<p>16. SUPPLEMENTARY NOTES</p>					
<p>17. KEY WORDS (Continue on reverse side if necessary and identify by block number) Multi-Function Sensor      Air Data Sensing Flight Control Sensor      Electric Field Sensing Rate Sensing      Magnetic Field Gradiometer Acceleration Sensing      Electric Field Gradiometer Magnetic Field Sensing</p>					
<p>18. ABSTRACT (Continue on reverse side if necessary and identify by block number) A two year development effort has culminated in flight-worthy test articles of multi-function sensors, for use in "strap-down" flight control systems. The multi-function sensor with one moving part, performs the equivalent to a two-axis rate gyro, two-axis linear accelerometer, a three-axis magnetic field sensor, a two-axis electric field sensor, and a two-axis air data probe. (over)</p>					

DD FORM 1 JAN 73 1473 EDITION OF 1 NOV 55 IS OBSOLETE

SECURITY CLASSIFICATION OF THIS PAGE (When Data Entered)

410 714



20. ABSTRACT (Continued)

Conclusions reached as a result of this development effort demonstrated the feasibility of a multi-function sensor which brings together the elements of a multi-mode flight control sensing scheme, that is, one which takes a measure of the earth's electric and magnetic fields, the air mass through which the carrying vehicle is moving, and a measure of vehicle angular velocity and linear acceleration. Its use is intended to determine vehicle heading, velocity, and attitude with respect to the magnetic north, air mass flow and local vertical. The thrust of the effort was to reduce cost, power consumption, volume and mechanical complexity by an order of magnitude.

A

aim

ii

## PREFACE

This report was prepared by Applied Devices Corporation, Kissimmee, Florida, Engineering, under U.S. Air Force Contract F33(615)-75-C-3154, initiated under USAF Project 1984, Task

The work was administered under the direction of the Control Systems Development Branch of the Flight Control Division, Air Force Flight Dynamics Laboratory, Air Force Systems Command, Wright-Patterson Air Force Base, Ohio by Van Roberts (AFFDL/FGL), Project Engineer.

This report covers work performed from March 1975 to February 1977. The project was directed by Roland Pittman. Special credit is tendered to Tom Dunn of the Control Systems Development Branch of the Flight Control Division, Air Force Flight Dynamics Laboratory, for his exceptional contribution to this project.

This report was submitted by the author in August 1977.

ACCESSION for	
NTIS	White Section <input checked="" type="checkbox"/>
DDC	Buff Section <input type="checkbox"/>
UNANNOUNCED	<input type="checkbox"/>
JUSTIFICATION.....	
BY.....	
DISTRIBUTION/AVAILABILITY CODES	
Dist.	AVAIL. and/or SPECIAL
A	

78 06 12 155

# TABLE OF CONTENTS

<u>Paragraph</u>		<u>Page</u>
<b>Section I</b>		
	<b>INTRODUCTION AND BACKGROUND</b>	<b>1</b>
1.1	Development History . . . . .	1
1.2	Program Objective . . . . .	1
1.3	Breadboard Hardware Objectives . . . . .	2
<b>Section II</b>		
	<b>SENSING TECHNIQUE DESCRIPTION</b>	<b>9</b>
2.1	Principles of Operation . . . . .	9
<b>Section III</b>		
	<b>GENERAL DESCRIPTION</b>	<b>15</b>
3.1	Construction . . . . .	15
3.2	Gas Motor Spin Drive . . . . .	15
3.3	Sensing Probes . . . . .	15
3.4	Rotor Assembly . . . . .	18
3.5	Sensor Outer Housing . . . . .	18
3.6	Purchased Components . . . . .	18
3.7	Overall Assembly . . . . .	22
3.8	Electronics Signal Processing . . . . .	22
<b>Section IV</b>		
	<b>TEST AND EVALUATION</b>	<b>29</b>
4.1	Test Setup Description . . . . .	29
4.2	Multi-Sensor Laboratory Tests Descriptions . . . . .	30
4.3	Test Results Summary and Conclusions . . . . .	34



## TABLE OF CONTENTS - Continued

<u>Paragraph</u>		<u>Page</u>
	Section V	
	PROTOTYPE GAS DRIVEN MULTI-SENSOR DESIGN AND PROJECTED COST DATA	41
	Section VI	
	CONCLUSIONS AND RECOMMENDATIONS	55
	Appendix A	
	MULTI-SENSOR SUMMARY TEST RESULTS	57
	Appendix B	
	ELECTRICALLY DRIVEN MULTI-SENSOR DEVELOPMENT	59
B.1	General . . . . .	59
B.2	Feasibility of Co-Functioning of the Magnetometer Probe With An Electro-Magnetic Spin Axis Drive Motor . . . . .	59
	Appendix C	
	GYRO STABILIZED ELECTRIC AND MAGNETIC FIELD EXPERIMENTAL SENSOR	71

# LIST OF ILLUSTRATIONS

<u>Figure</u>		<u>Page</u>
1	Multi-Function Sensing Technique for Flight Control . . . . .	3
2	Modular Adaptive, Variable Function Flight Control Sensor--Projected Costs (Unburdened) .	4
3	Multi-Function Sensing Geometry . . . . .	10
4	Signal Format . . . . .	14
5	Multi-Sensor (Gas Driven Design) . . . . .	16
6	Slipring/Shaft to Sensing Probe Assembly . . . . .	17
7	Rate Sensing Probe Design Details . . . . .	19
8	Linear Acceleration Probe Design Details . . . . .	20
9	Air Mass Probe Design Details . . . . .	21
10	Reference Generator Design Data . . . . .	23
11	Electric Field Probe Design . . . . .	25
12	Isolation Preamplifier--Nonmagnetic Construction .	26
13	Multi-Sensor Internal Schematic . . . . .	28
14	Prototype Multi-Function Sensor (Gas Driven) . . .	43
15	Multi-Sensor Housing Assembly Molded Configuration	44
16	Multi-Sensor Rotor Assembly Molded Configuration .	45
17	Multi-Sensor Signal Conditioning Module Schematic .	51
18	Strapdown, All Attitude, Heading and Attitude Reference System Comparison (Cost) . . . . .	53
19	Strapdown, All Attitude, Heading and Attitude Reference System Comparison (Complexity) . . .	54
B-1	Electrically Driven Multi-Sensor . . . . .	60
B-2	Electrically Driven Multi-Sensor Schematic Diagram .	61
B-3	Distortion of Field (Induction Effects) . . . . .	62
B-4	Electro/Magnetic Spin Motor Noise Sources/Effects on Simple Coil Probe--Motor Excitation Losses .	63
B-5	Electro/Magnetic Spin Motor Noise Sources/Effects on Simple Coil Probe--Inter-Field Reflective Effects . . . . .	65
B-6	Electro/Magnetic Spin Motor Noise Sources/Effects on Modulated Magnetic Flux Type Probe--X/Y Axis Configuration . . . . .	66
B-7	Modulated Magnetic Flux Type Probe Test Bed (Tracking Accuracy) . . . . .	67
B-8	Signal Detection . . . . .	69
C-1	Gyro Stabilized Electric and Magnetic Field Sensor .	72
C-2	Gimbal Angle Transducing Scheme . . . . .	73

# LIST OF TABLES

<u>Table</u>		<u>Page</u>
1	Multi-Mode Sensor Performance Goals . . . . .	5
2	Spin Axis Bearing Setup Data . . . . .	24
3	Threshold and Speed Regulation Tests Using 9-in. Hg Venturi No. 2 . . . . .	30
4	Multi-Sensor: H.O.G. No. 2 Performance Problems . . . . .	36
5	Multi-Sensor Performance Summary . . . . .	38
6	Multi-Function Sensor Molding Material Fiberite 4004 . . . . .	46
7	Multi-Mode Sensor Compression Transfer Molding Tooling Estimates . . . . .	47
8	Multi-Mode Sensor Molded Parts Cost Projections . . . . .	48
9	Multi-Mode Sensor Overall Tooling Cost Projections . . . . .	49
10	Multi-Mode Sensor Cost Projections (Bare Costs) . . . . .	50
11	Signal Conditioning Module Schematic Outline .	52
A-1	Multi-Sensor Summary Test Results . . . . .	57
C-1	Gimbal Pickoff Performance Test Data . . . . .	74



## SUMMARY

A two year development effort has culminated in flight worthy test articles of multi-function sensors, for use in "strap-down" flight control systems. The multi-function sensor with one moving part, performs the equivalent of a two-axis rate gyro, a two-axis linear accelerometer, a three-axis magnetic field sensor, a two-axis electric field sensor, and a two-axis air data probe.

Conclusions reached as a result of this development effort demonstrated the feasibility of a multi-function sensor which brings together the elements of a multi-mode flight control sensing scheme, that is, one which takes a measure of the earth's electric and magnetic fields, the air mass through which the carrying vehicle is moving, and a measure of vehicle angular velocity and linear acceleration. Its use is intended to determine vehicle heading, velocity, and attitude with respect to the magnetic north, air mass flow and local vertical. The thrust of the effort was to reduce cost, power consumption, volume and mechanical complexity by an order of magnitude.

## SECTION I

### INTRODUCTION AND BACKGROUND

#### 1.1 DEVELOPMENT HISTORY

In March of 1975, Applied Devices Corporation was awarded Air Force Contract F33615-75-C-3154 to develop feasibility demonstration models of a multi-function sensor to be used primarily in the body-mounted mode for stability augmentation, and flight heading and attitude reference systems. This sensing technique, which results in combined outputs for magnetic heading, vertical referencing and air data, was in general accordance with Applied Devices Corporation's proposal dated February 24, 1975 entitled "Modular Adaptive, Variable Function, Flight Control Sensor."

This work was built on a technology base developed under earlier contracts with the Flight Dynamics Laboratory, and on certain research and development accomplished by the author while in tenure at Wright-Patterson Air Force Base as a consultant.

Significant accomplishments which were the result of this research and development effort included the following:

- 1) Feasibility was clearly demonstrated for an ultra low cost multi-function sensor for flight control applications.
- 2) A high accuracy magnetic compass transmitter technique was demonstrated.
- 3) A new air data sensing concept was demonstrated.
- 4) A compass transmitter suitable for application in a magnetically noisy environment was demonstrated.
- 5) A "directly" gyro stabilized magnetic compass was demonstrated.
- 6) The possibility for a new air-to-air terminal aid was demonstrated.

#### 1.2 PROGRAM OBJECTIVE

The program objective was to demonstrate the feasibility of the multi-function sensor concept in terms of the following design characteristics:

- 1) Modular design.

- 2) One overall design through mixes of primary sensors to measure many parameters (needs no redesign).
- 3) Design amenable to plastic fabrication techniques.

The specific task was to bring together the elements of a multi-mode flight control sensing scheme, that is, one which takes a measure of the earth's electric and magnetic fields, the air mass through which the carrying vehicle is moving, and a measure of vehicle angular velocity and linear acceleration. Its use was intended to determine vehicle heading, velocity, and attitude with respect to the magnetic north, air mass flow and local vertical. The thrust of the effort was to reduce cost, power consumption, volume and mechanical complexity by an order of magnitude or more; this technique allows two body-mounted sensors to supply all of the sensed data, as summarized in Figure 1.

The realization of these objectives results in important payoffs in the following ways:

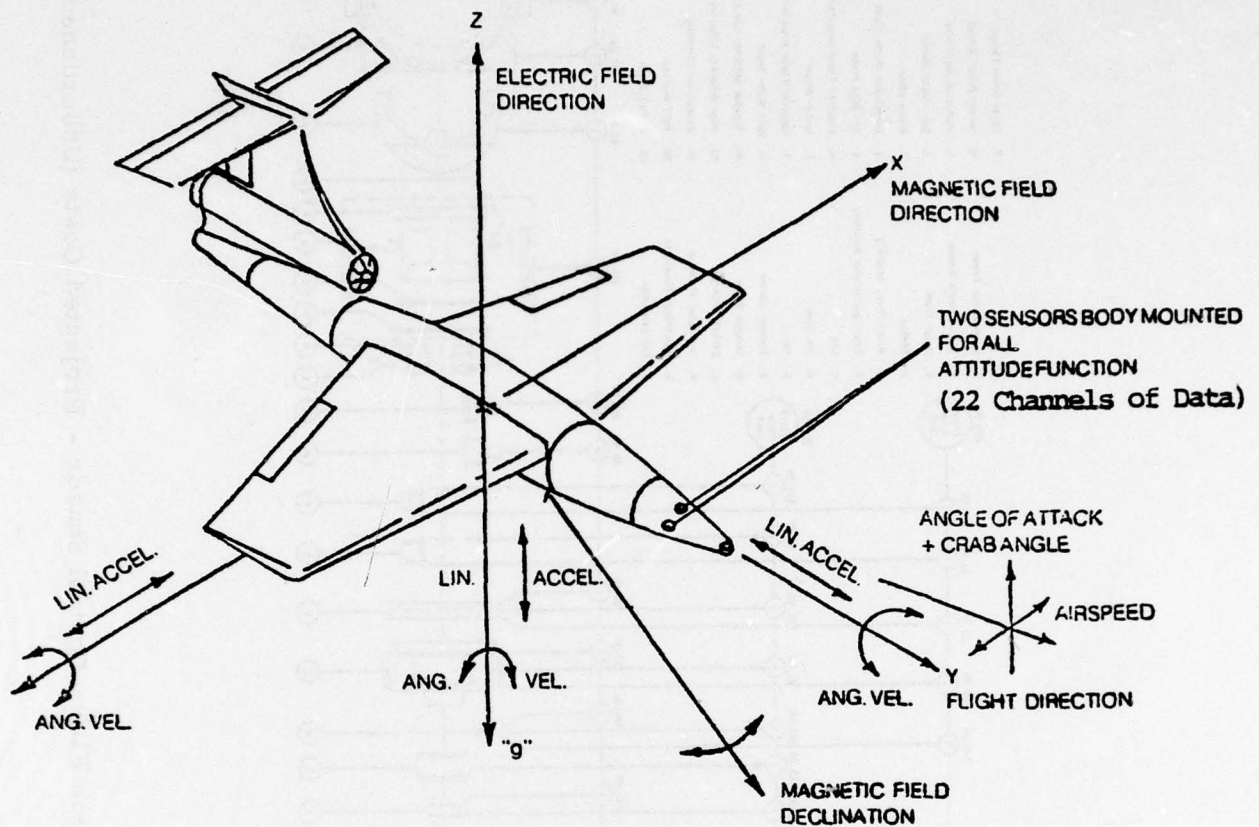
- Absolute weight, volume, and power supply requirements, which are now a significant part of RPV payload, are improved.
- Installation and harnessing complexity is reduced.
- Mechanical joints, which are weak links, are greatly improved, thus improving reliability.
- The cost of ownership is reduced, due to a reduction in the number of high cost devices in the inventory (modular design).
- There is a direct unit replacement savings for first 1,000 units.

### 1.3 BREADBOARD HARDWARE OBJECTIVES

The specific hardware objectives for the breadboard development effort were broadly dictated by the proof of cost and performance. A summary of the goals in these two areas is given in Figure 2, and Table 1. The detailed steps in the development effort to achieve these goals included:

- 1) Designing, building, and testing two sensor samples with all the probes in combination to provide proof of feasibility.





### FEATURES

- Multiple Axis Sensing: ~~Eleven~~ Outputs
- High Reliability: Only one moving part
- Miniaturized: Low mass
- Low Power Consumption
- Low Cost: One sensor replaces many
- Simple Installation: Body mounted
- Gas or Electric Spin Drive
- Modular, Adaptive

Figure 1. Multi-Function Sensing Technique for Flight Control.

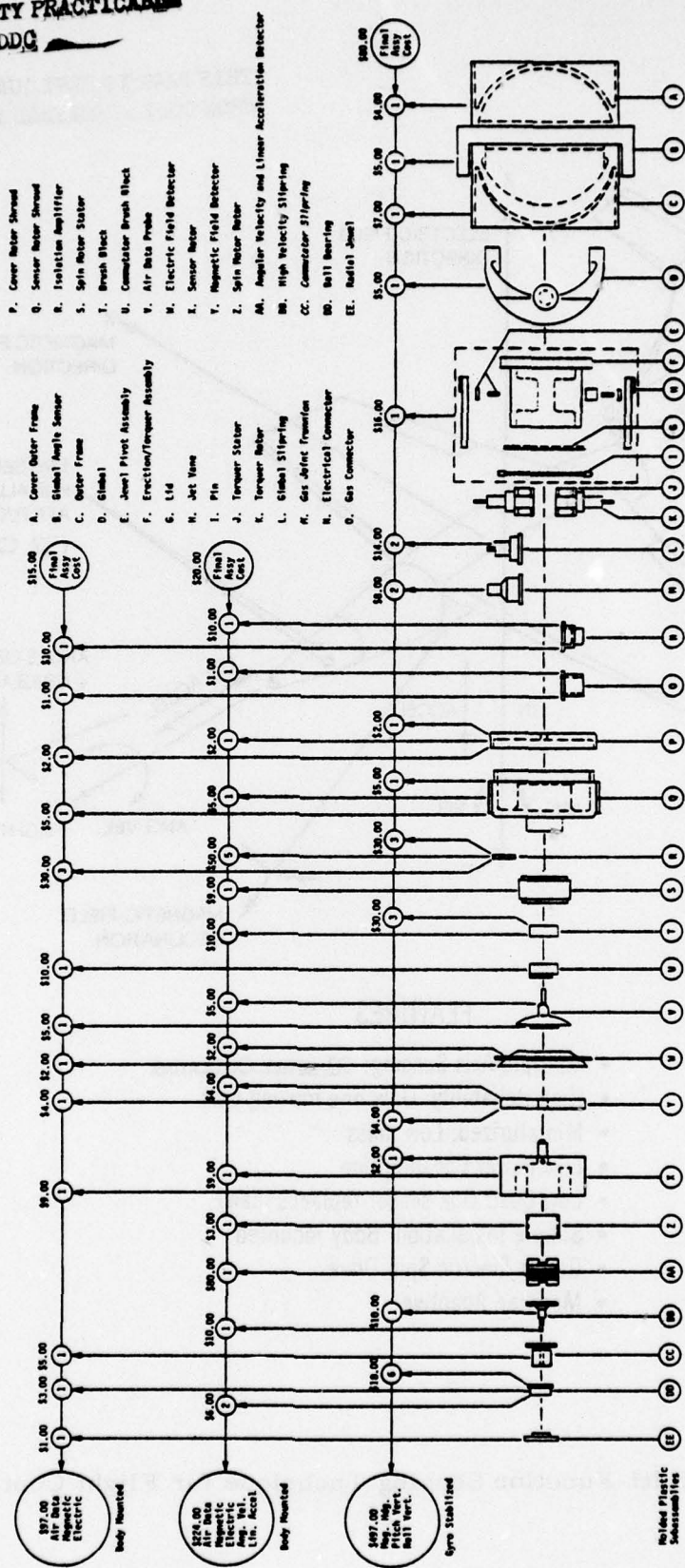


Figure 2. Modular Adaptive, Variable Function Flight Control Sensor - Projected Costs (Unburdened).

TABLE 1. MULTI-MODE SENSOR PERFORMANCE GOALS

Parameters	I Magnetometer	II Electrometer	III Air Data Meter	IV Angular Velocimeter		V Linear Accelerometer
				Angular	Velocimeter	
1. Nominal Reference Inputs	0.3 Gauss	150 V/m	250 m.p.h.	1 deg./sec.	1 "g"	
2. Scale Factor	10 V/Gauss	0.017 V/Vm	0.010 V/m.p.h.	0.017 V/deg/sec.	0.250 V/"g"	
3. Signal Amplification	X1000.0	X100.0	X10.0	X10	X1.0	
4. Maximum Bias	1 x10 <sup>-3</sup> Gauss	3 V/m	5 m.p.h.	15 deg./hr.	5 x10 <sup>-3</sup> "g"	
5. Threshold*	1 x10 <sup>-4</sup> Gauss	0.1 V/m	0.5 m.p.h.	1 deg./hr.	1x10 <sup>-4</sup> "g"	
6. Null Uncertainty (Dynamic)	3 x10 <sup>-4</sup> p-p	0.3 V/m p-p	1.5 m.p.h. p-p	3 deg/hr. p-p	5x10 <sup>-4</sup> "g" p-p	
7. Null Uncertainty (hr. to hr.)	2 x10 <sup>-4</sup> r.m.s.	0.2 V/m r.m.s.	1.0 m.p.h. r.m.s.	0.5 deg/hr. r.m.s.	2x10 <sup>-4</sup> "g" r.m.s.	
8. Null Uncertainty (Turn-On to Turn-On)	5 x10 <sup>-4</sup> p-p	0.5 V/m r.m.s.	1.5 m.p.h. r.m.s.	3 deg./hr. p-p	1x10 <sup>-3</sup> "g" p-p	
9. Linear Operating Range	0.5 Gauss	300 V/m	500 m.p.h.	300 deg./sec.	20 "g"	
10. Maximum Over Range Input	10 Gauss	1000 V/m	1000 m.p.h.	600 deg./sec.	100 "g"	
11. Linearity	±2%	±2%	±1 %	±0.5%	±0.25%	
12. Symmetry	1 %	1 %	1 %	1 %	1 %	
13. Settling Time (Response to Step Input)	0.1 sec.	0.1 sec.	0.01 sec.	0.001 sec.	0.0005 sec.	

\*The smallest signal level which is accurate to within ±50% of the proper value as referred to the nominal scale factor.



TABLE 1. MULTI-MODE SENSOR PERFORMANCE GOALS - CONTINUED

Parameters	I Magnetometer	II Electrometer	III Air Data Meter	IV Angular Velocimeter	V Linear Accelerometer
14. Cross Axis Coupling (Steady State)	$\pm 1\%$	$\pm 2\%$	2 %	1 %	0.2%
15. Inter-Axis Alignment	$\pm 0.25$ deg.	$\pm 0.25$ deg.	0.25 deg.	$\pm 0.15$ deg.	$\pm 0.05$ deg.
16. Cross Quantity Alignment	$\pm 0.2$ deg.	$\pm 0.2$ deg.	$\pm 0.2$ deg.	$\pm 0.1$ deg.	0 deg. (ref.)
17. Cross Quantity Coupling					
I. Magnetic Field	100%	Insignificant	Insignificant	Insignificant	Insignificant
II. Electric Field	Insignificant	100%	Insignificant	Insignificant	Insignificant
III. Air Mass Flow	Insignificant	Prone to Install Effects	100%	0.001 deg./hr. / m.p.h.	$1 \times 10^{-6}$ "g"/m.p.h.
IV. Angular Velocity	$1 \times 10^{-5}$ Gauss / deg./sec.	0.005 V/m/deg./sec.	0.01/m.p.h./deg./sec	100%	$1 \times 10^{-4}$ "g"/deg./sec.
V. Linear Acceleration	Insignificant	Insignificant	0.1 m.p.h./"g"	3 deg./hr./"g"	100%

- 2) Building, testing, and demonstrating a block of prototype multi-function sensors to evaluate nominal performance and gather cost data.
- 3) Performing a detailed analysis of cost trade-offs between molded fabrication vs. automatic screw machine approaches.
- 4) Carrying out research and development into the feasibility of electrically driven magnetometers.
- 5) Conducting a field test series to determine the applicability of the electro-meter portion of the multi-sensor as a sensor for an air-to-air terminal aid.

## SECTION II

### SENSING TECHNIQUE DESCRIPTION

#### 2.1 PRINCIPLES OF OPERATION

This sensing scheme utilizes rotating probes suitably configured to detect the various forcing functions arising from the input phenomenon. Specifically, each operates to convert a quasi steady state input into a suppressed carrier modulated output signal. This results in a measure of the amplitude and direction of the total vector of that input lying in the sensing plane, as determined by the spin axis of the rotating probe. Referring to Figure 3, the various sampling probes are shown schematically, and include the magnetic field, electric field, air mass flow, linear acceleration and angular velocity. Common characteristics of the sensing scheme have to do with the means needed to rotate the probe assembly, transmit information across the spinning gap, and structure it. In addition, a common reference generator is required to resolve the two orthogonal axis components of sensed signal lying in the plane of rotation.

With one rotating part, this technique yields the measurement of the equivalent of 11 single-channel conventional transducers, with potentially the electro mechanical complexity and cost of a typical single unit. To consider each of the sensing probes, the following descriptions are presented.

#### X/Y MAGNETIC FIELD SENSING PROBE

To sense the magnetic field, a transducing technique is used which measures the field drop across the physical dimensions of the sensor. This is accomplished by arranging a rotating closed loop conductor in such a fashion as to cut the incident flux at right angles to the spin axis. A sine wave signal is generated which has frequency identical to the spin period, for that condition where the field is linear.

For an incident magnetic field which is not colinear, i.e., contains a gradient, harmonics of the fundamental are generated. In the simple case, the second harmonic would be the most dominant. In effect, the main field and gradient fields give uniquely different signal frequencies.



THIS PAGE IS BEST QUALITY PRACTICABLE  
FROM COPY FURNISHED TO DDG

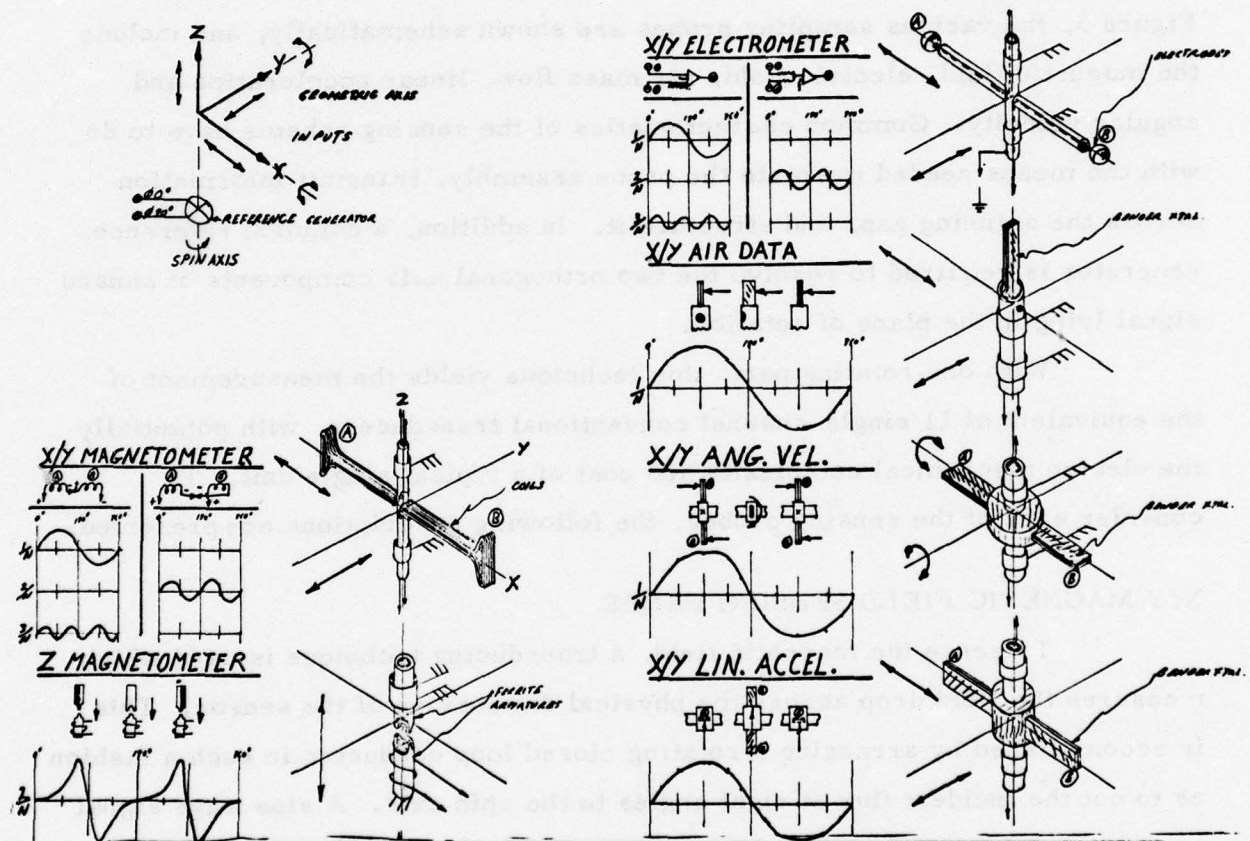


Figure 3. Multi-Function Sensing Geometry.

Referring to Figure 3, the X/Y magnetrometer sensing probe consists of two identical coils with the outer ends so arranged as to cut the incident field at a right angle to the spin axis, and the radial returns of the coils flattened and so positioned with respect to the spin axis that the axial return is near the center of rotation. This gives the section lying at the major radius most of the charge generating capacity for the probe.

For one combination of polarities, the two probes are in common mode rejection for the fundamental and odd harmonics, and in the opposite sense, common mode rejection for the even harmonics. The interesting property of this geometry is the capacity of the sensing probe to essentially ignore an ungraded field.

For the case at hand, the probe is interconnected to sense the "main" field.

#### Z AXIS MAGNETOMETER PROBE

Referring to Figure 3, the Z axis probe consists of two identical ferrite members, one on the rotor and one fixed to the frame in juxtaposition, such that a tooth detail is presented which significantly changes the gap twice per spin revolution. This operates to modulate the magnetic reluctance at twice spin frequency, thereby generating in the coil wound around the fixed rod, currents proportional to the flux in the gap. The length-to-diameter ratio of the ferrite rods is such that they essentially act as flux conductors, tending to concentrate the field along the spin axis, in the gap. The ferrite material is selected on the basis of its low retentivity and relatively high permeability.

#### X/Y AXIS ELECTROMETER PROBE

The X/Y electrometer operates geometrically in a way similar to that described for the X/Y magnetometer. The sensor probe for the electric field consists of a shielded rotating dipole terminated with exposed electrodes depicted in the diagram as spheres. Its operation is essentially equivalent to

that of a conductive surface translating through the electric field, the difference being that the conductor changes its direction periodically at the spin frequency, thereby resulting in a dynamic output proportional to field strength. By measuring the output of the balanced dipole in one sense, the fundamental and odd harmonics are obtained, and in the inverted sense the even harmonics result.

#### X/Y AIR DATA PROBE

The air mass data probe is a small area flat plate rotating at a right angle to the sensing plane, coupled to a piezoelectric generator, which simultaneously becomes the restoring spring and signal generator. Its operation is one where, for a steady state gas flow impinging upon the rotating flat plate, an oscillating force is exerted on the crystal restraint. This gives a measurement of total vector direction and amplitude of the air mass flow with respect to the sensor mount. For two cases of location and attitude of the sensor installation on the vehicle, it senses air speed and crab angle or air speed and angle of attack. The third case measures crab angle and angle of attack.

#### X/Y AXIS ANGULAR VELOCITY

The angular velocity probe is based on the gyroscopic operation of an elastically restrained body rotating at high velocities. In the case at hand, a piezoelectric crystal functions simultaneously as the inertial member and the restoring spring. Typically, two bender crystals are arranged in a dipole fashion for common mode rejection and inertial balance. The operation is such that the angular momentum of the masses, reacting as a result of an applied angular velocity at right angles to the spin axis, generates a forcing function which is sinusoidal in distribution and exhibits a frequency identical to that of the spin axis, with output amplitude proportional to the applied input.

#### X/Y AXIS LINEAR ACCELERATION PROBE

The acceleration measurement is achieved by an arrangement of bender crystals similar to that of the rate section, except that the crystals' sensitive axes have been turned 90° to react to acceleration parallel to the



spin plane. In addition, the two crystals are electrically interconnected in the opposite sense from that of the rate section to give an additive output for the two elements.

Under steady state acceleration, the rotation of the crystal array will cause a sinusoidal voltage to be developed at the output when it is interconnected in the additive mode.

#### REFERENCE GENERATOR

In order to determine the direction of the various input phenomenon as sensed by the probes, it is necessary to have a reference signal to which the outputting signals can be compared to make a coordinate conversion from the rotating frame to the fixed frame. This is accomplished by a spin axis reference generator configured with two  $90^\circ$  phase-shifted outputs, with their null points aligned accurately to alignment surfaces on the sensor's outer case. Using these reference signals in conjunction with the various probe outputs, it is then possible to determine the direction and amplitude in terms of the body axis coordinates.

The signal conditioning required to resolve the data from the rotating to the fixed frame reference and resulting in a polarity sensitive d.c. output is shown in Figure 4.

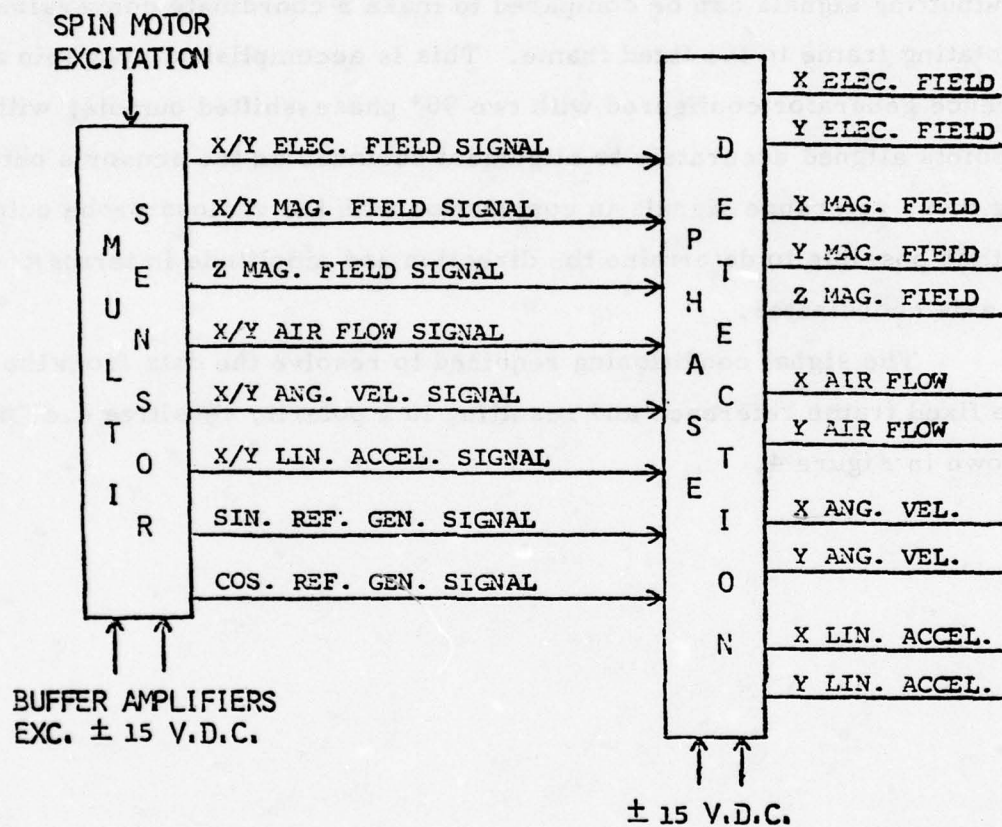


Figure 4. Signal Format.

## SECTION III

### GENERAL DESCRIPTION

The general design and assembly arrangements for the initial brass-board effort can be recognized in Figure 5, which uses machined plastic construction throughout.

#### 3.1 CONSTRUCTION

The material, in general, is glass reinforced epoxy plastic. All of the end bells for the rotor and outer housing are fabricated from standard .062-in. thick P.C. board material. The glass reinforced epoxy printed circuit board material works very well in the design, in terms of achieving low cost material covering for electrical shielding.

#### 3.2 GAS MOTOR SPIN DRIVE

The gas motor is essentially the same as that used in standard gas driven gyros, whose performance is quite predictable. The spinup time to 200 Hz with a standard gas supply of 3.2 in. of mercury is approximately 1 1/2 minutes.

#### 3.3 SENSING PROBES

The X/Y magnetometer probe consists of two bobbins separately wound with 1200 turns of wire mounted on a carrier centerpiece constructed of reinforced glass epoxy and terminated. The interconnections are made internally for common mode rejection to give an output for the main field and odd harmonics. This begins the subassembly of the rotating element and with the addition of the shaft and slip ring forms the reference for all subsequent alignments for the rotor (see Figure 6).

The rate and acceleration sensing probes are built as separate subassemblies and typically consist of a center hub made of plastic with terminals onto which two bender crystals are fastened, using suitable alignment fixturing. These two separate subassemblies, having been tested for



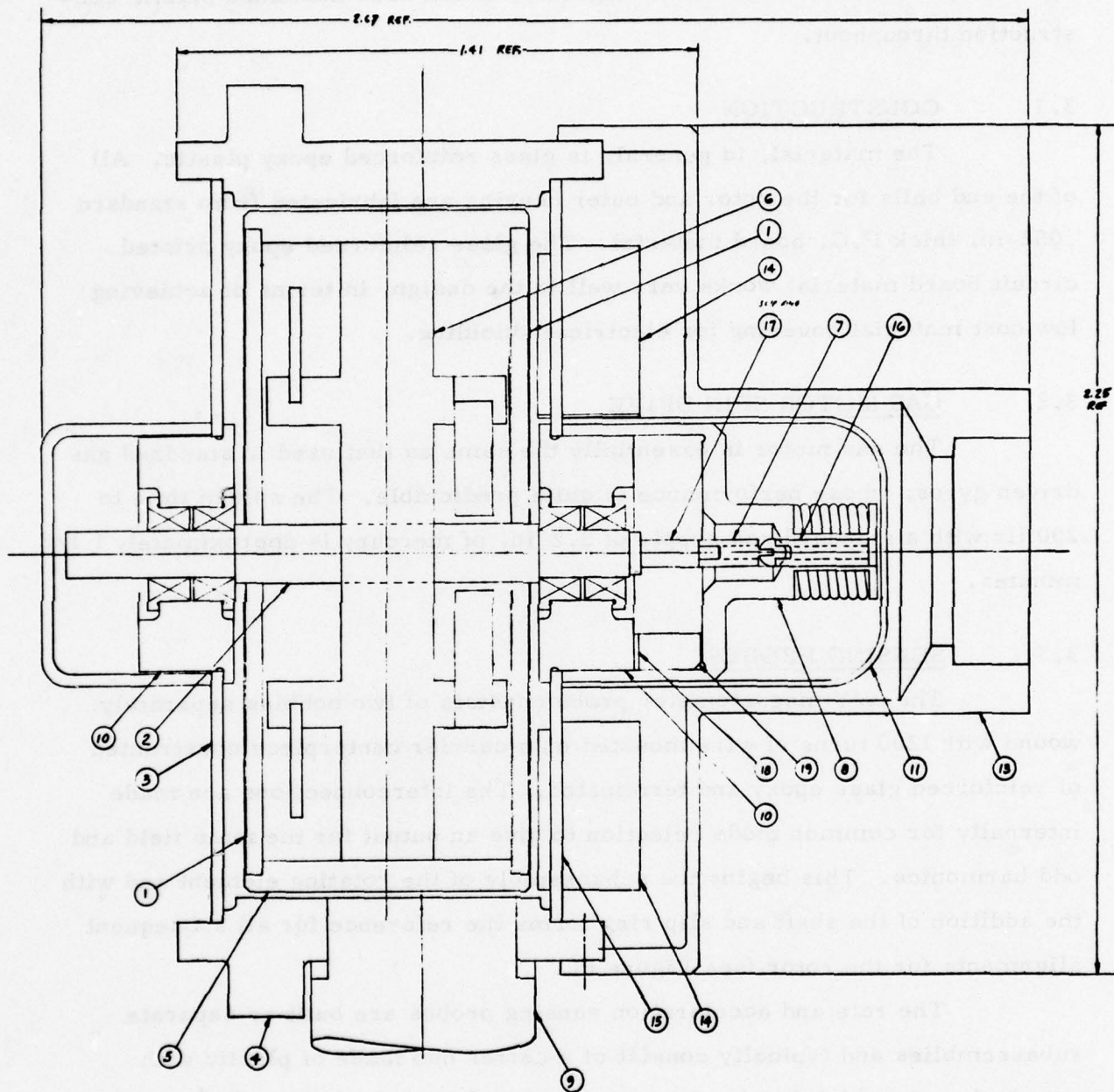
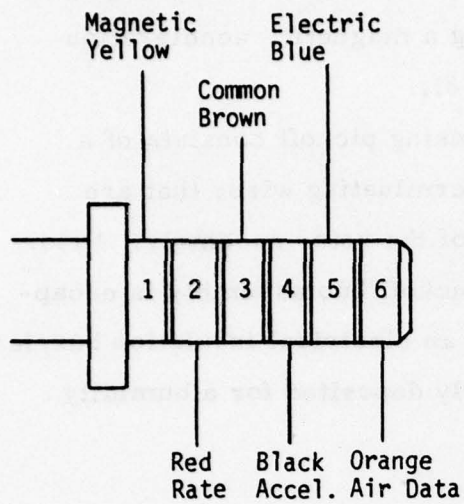


Figure 5. Multi-Sensor (Gas Driven Design).



Magnetic Field Coil  
Resistance =  $675\ \Omega$   
1,400 Turns = No. 42 A.W.G. Wire

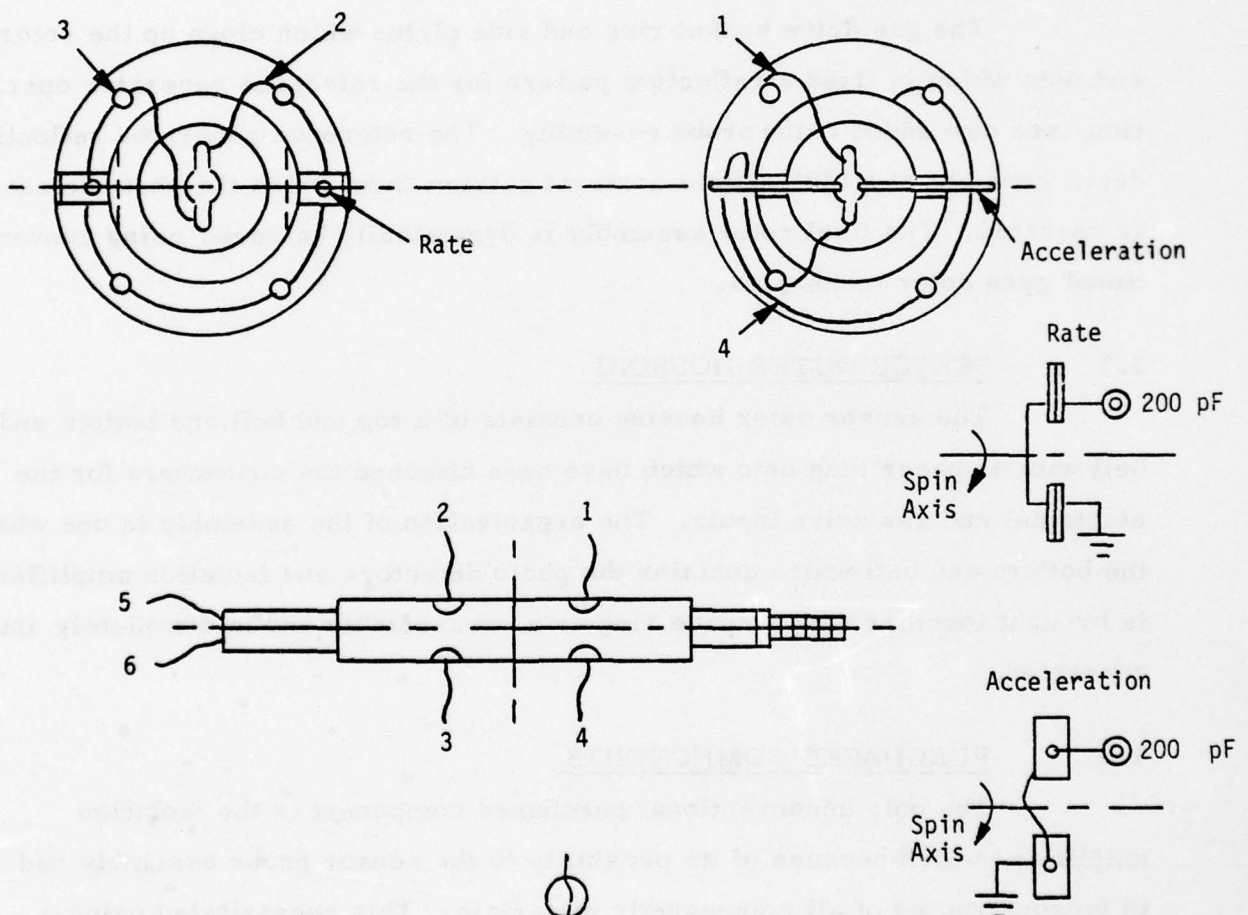


Figure 6. Slipring/Shaft to Sensing Probe Assembly.

scale factors and natural frequency on a vibration fixture, are then brought to the shaft magnetometer assembly, thus forming a magnetic, acceleration and rate sensing subassembly (see Figures 7 and 8).

Referring to Figure 9, the air data sensing pickoff consists of a bender bymorph crystal molded into a base with terminating wires that are interconnected with the slip ring at the other end of the rotor assembly. Prior to installation in the spin axis shaft, the crystal pickoff hub assembly is encapsulated with a thin layer of flexible epoxy to form an electrical insulation barrier, with a subsequent thin coating of nickel electrolytically deposited for a humidity barrier and electrostatic shield.

#### 3.4 ROTOR ASSEMBLY

The gas drive bucket ring and side plates which close up the rotor, and onto which is fixed a reflective pattern for the reference generator operation, are now added to the probe assembly. The reference generator reflective detail consists of a 180° optical contrast pattern from which the photo detector is operated. The final rotor assembly is dynamically balanced using conventional gyro rotor techniques.

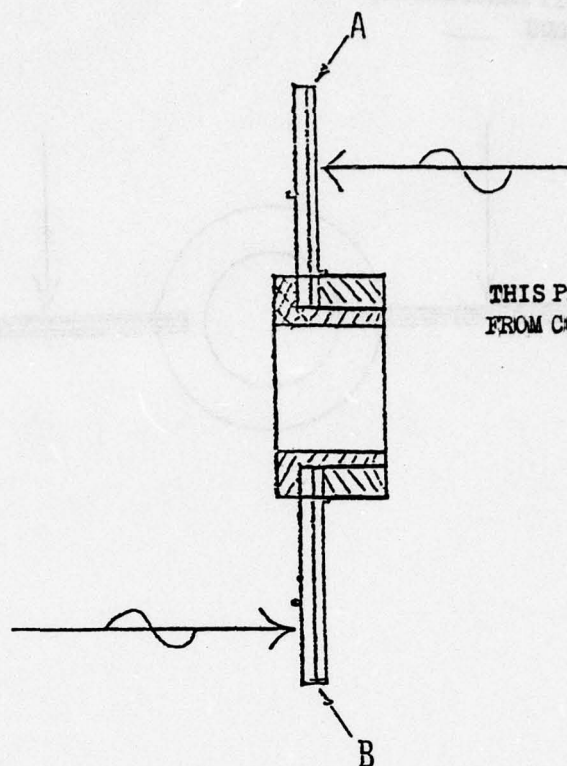
#### 3.5 SENSOR OUTER HOUSING

The sensor outer housing consists of a top end bell and bottom end bell with a spacer ring onto which have been attached the connectors for the electrical and gas drive inputs. The organization of the assembly is one where the bottom end bell which contains the photo detectors and isolation amplifiers is brought together with a space ring as a subassembly and is completely interconnected.

#### 3.6 PURCHASED COMPONENTS

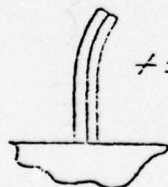
The only unconventional purchased component is the isolation amplifier, which because of its proximity to the sensor probe assembly had to be constructed of all nonmagnetic materials. This necessitated using a special packaging technique furnished by the Mini Systems Corporation of North Attleboro, Massachusetts. The slip rings and brush block assemblies were





THIS PAGE IS BEST QUALITY PRACTICABLE  
FROM COPY FURNISHED TO DDC

CRYSTAL SENSING  
POLARITY



$\div$  = COMPRESSIVE

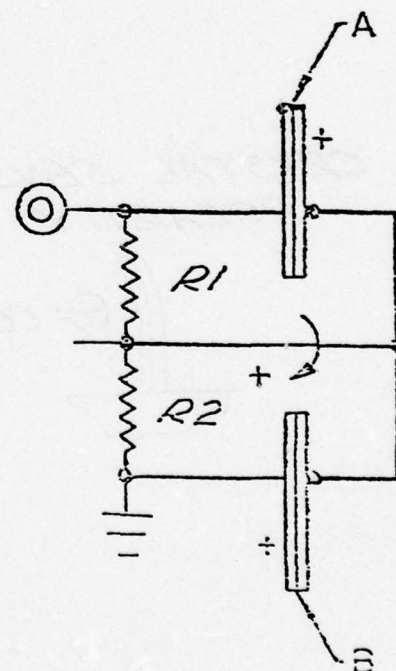
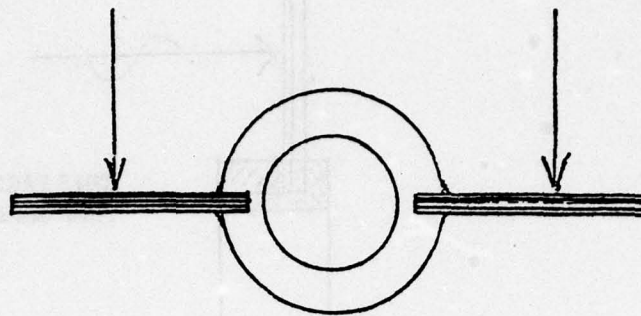


Figure 7. Rate Sensing Probe Design Details.

THIS PAGE IS BEST QUALITY PRACTICABLE  
FROM COPY FURNISHED TO DDC



CRYSTAL SENSING  
POLARITY

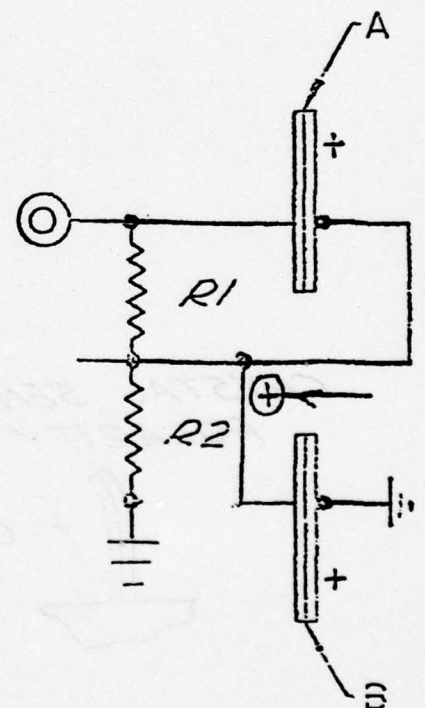
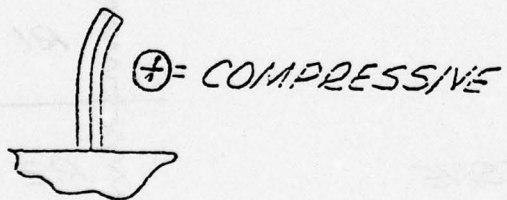


Figure 8. Linear Acceleration Probe Design Details.

THIS PAGE IS BEST QUALITY PRACTICABLE  
FROM COPY FURNISHED TO DDG

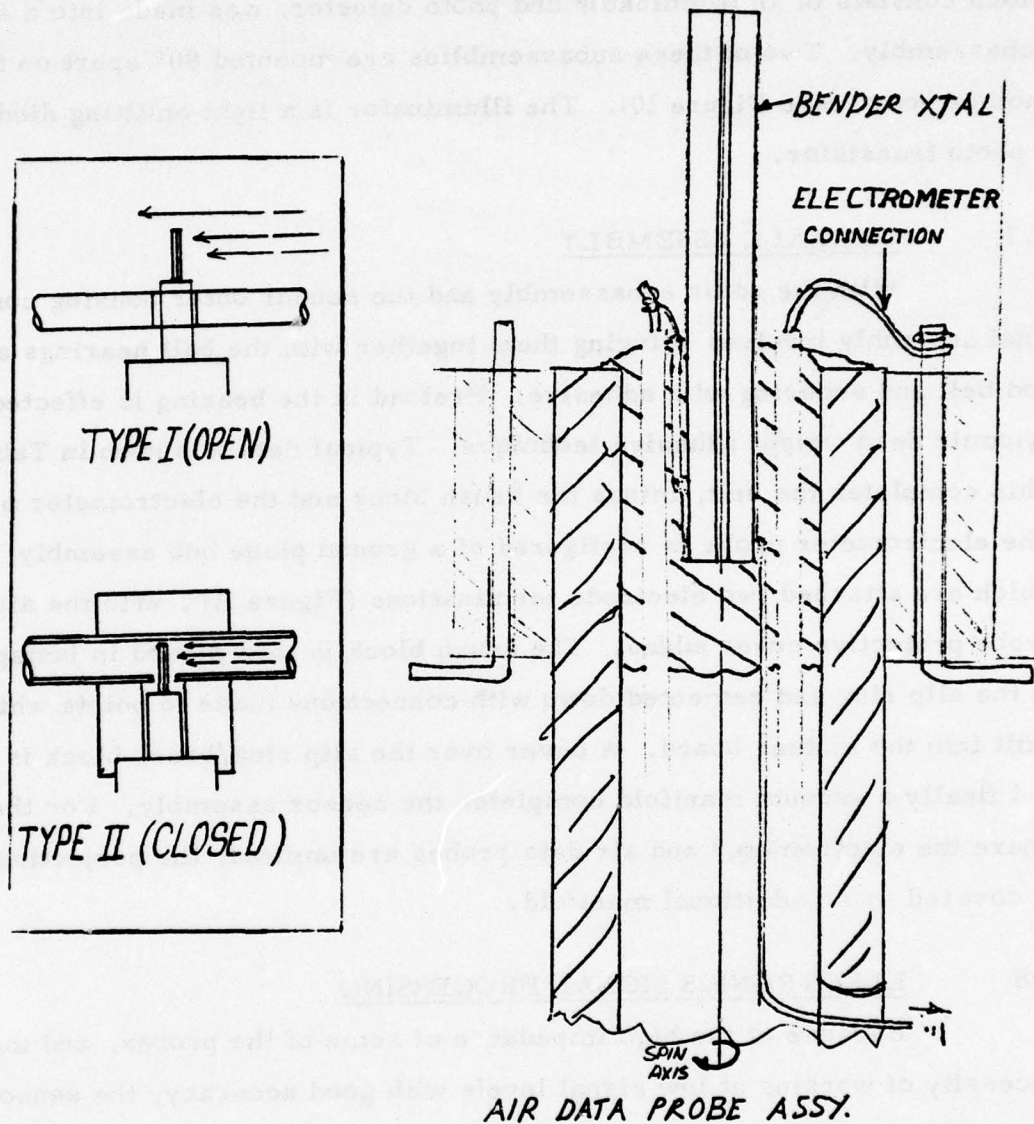


Figure 9. Air Mass Probe Design Details.



procured from Poly Scientific Corporation in Blacksburg, Virginia, and were essentially off-the-shelf. That is, the tooling was already developed. The ball bearings are standard high precision miniature type R144 procured from the Bardon Corporation in Danbury, Connecticut. The reference generator, which consists of an illuminator and photo detector, was made into a separate subassembly. Two of these subassemblies are mounted 90° apart on the mother board (see Figure 10). The illuminator is a light emitting diode driving a photo transistor.

### 3.7 OVERALL ASSEMBLY

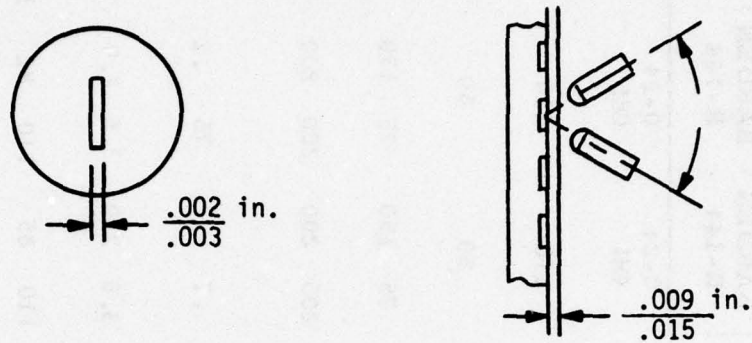
With the rotor subassembly and the sensor outer housing complete, final assembly involves bringing them together with the ball bearings and top end bell and securing with adhesive. Preload in the bearing is effected by a dynamic dead weight adhesive technique. Typical data is shown in Table 2. This completes the unit, minus the brush block and the electrometer probe. The electrometer probe is configured of a ground plane hub assembly, onto which are attached two electrode terminations (Figure 11), with the air data probe protective cover added. The brush block is then placed in juxtaposition to the slip ring and cemented down with connections made to points which are built into the mother board. A cover over the slip ring/brush block is added, and finally a vacuum manifold completes the sensor assembly. For the case where the electrometer and air data probes are omitted, the projecting shaft is covered by an additional manifold.

### 3.8 ELECTRONICS SIGNAL PROCESSING

Because of the high impedance of some of the probes, and the necessity of working at low signal levels with good accuracy, the sensor requires integrally mounted isolation amplifiers.

The isolation preamplifiers, as shown in Figure 12, are in turn mounted to a mother board which becomes integrally connected to the sensor assembly, and as such, is a completely wired and potted subassembly. Also

- (1) Excitation \_\_\_\_\_ LED .040 A
- (2) Detector \_\_\_\_\_ Photo-Transistor
- (3) Reflective Disc \_\_\_\_\_ Aluminum/Alumina
- (4) 128-Cycle Pattern, With 50% Contrast Duty Cycle



- (5) Output \_\_\_\_\_ .25/.50 V Peak
- (6) Offset \_\_\_\_\_ <.25 V

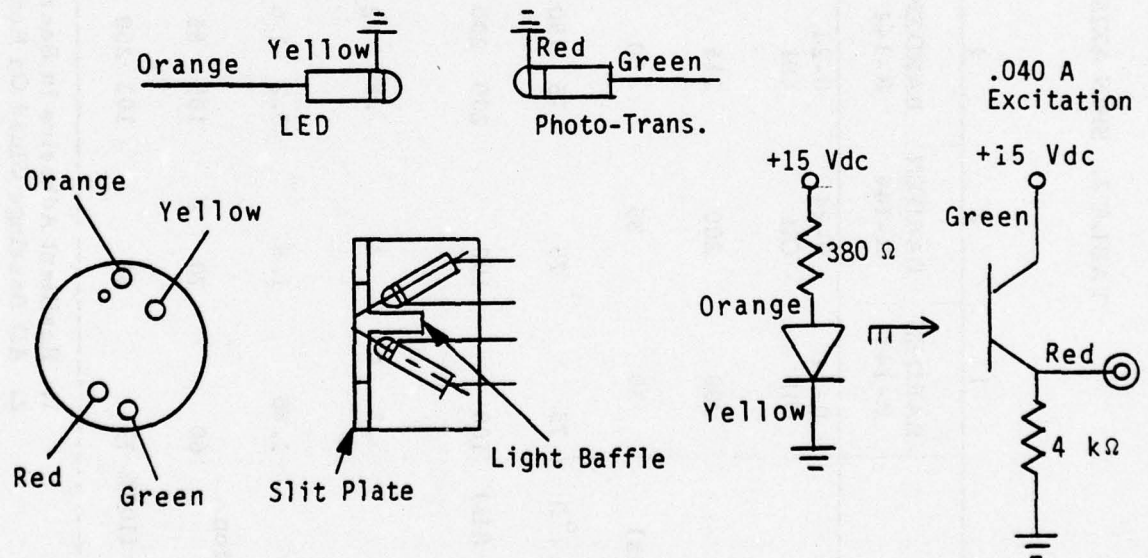


Figure 10. Reference Generator Design Data.

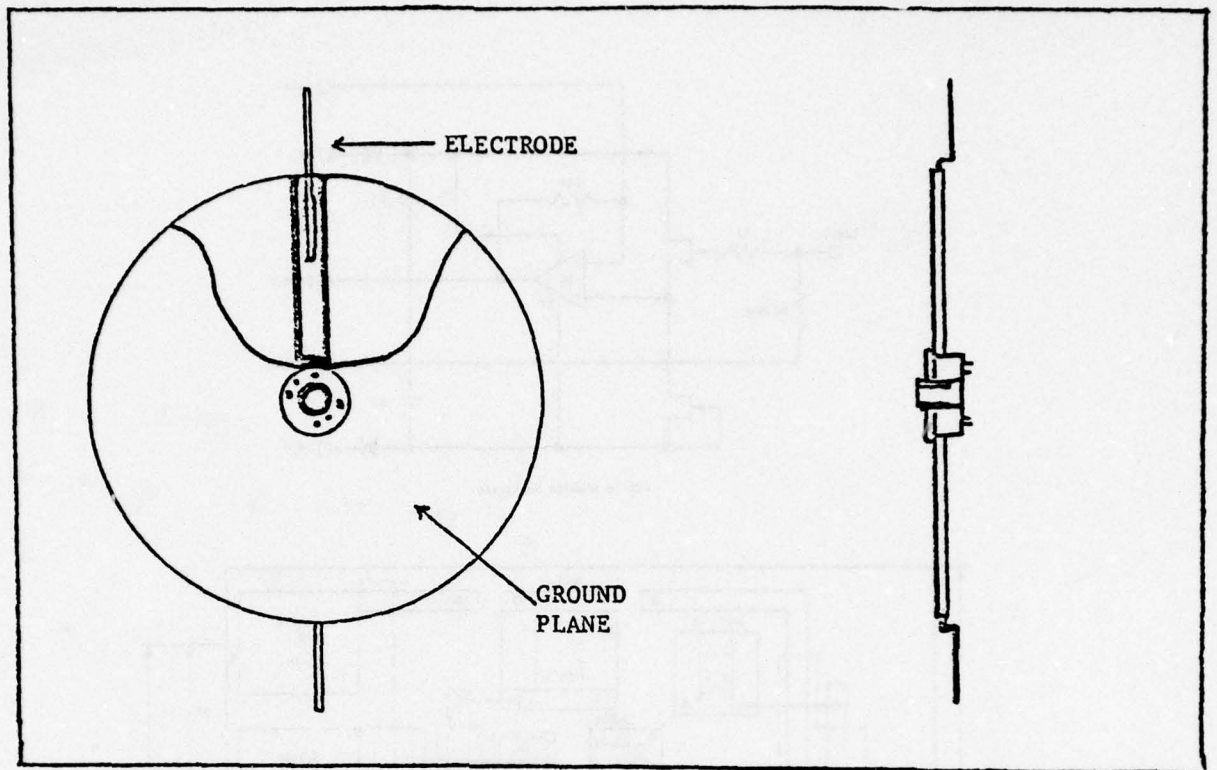
TABLE 2. SPIN AXIS BEARING SETUP DATA

Parameters	Units													
	1	2	3	4	5	6	7	8						
Bearing Type	BARDEN R-144	BARDEN R-144	BARDEN R-144	BARDEN R-144	BARDEN R-144	BARDEN R-144	BARDEN R-144	BARDEN R1-5H						
Lubrication	0-24 Oil	0-24 Oil	0-24 Oil	0-24 Oil	0-24 Oil	0-24 Oil	0-24 Oil	G-2 Grease						
Preload (Grams)	200	200	315	210	210	210	210	210						
Rotor Mass (Grams)	35	35	50	50	50	50	50	50						
Temperature Data ( <sup>o</sup> f)	75	75	75	150	75	150	75	150						
Terminal Velocity (Hz)	100	100	200	200	200	200	200	200						
Starting Pressure (Hg., In.)	.3	.2	.8	.2	.8	.3	.7	.2	.75	.2	.6	.3	.9	.3
Running Pressure (Hg., In.)	1.85	1.8	3.2	2.6	3.7	2.8	3.8	2.9	3.5	2.9	3.4	2.6	4.4	3.45
Time to Acceleration (Sec.) (90%)	60	70	105	85	115	85	110	85	110	82	103	90	120	85
Coast Time (Sec.) (100%, 75	75	80	103	260	160	350	180	370	175	360	197.5	380	150	300

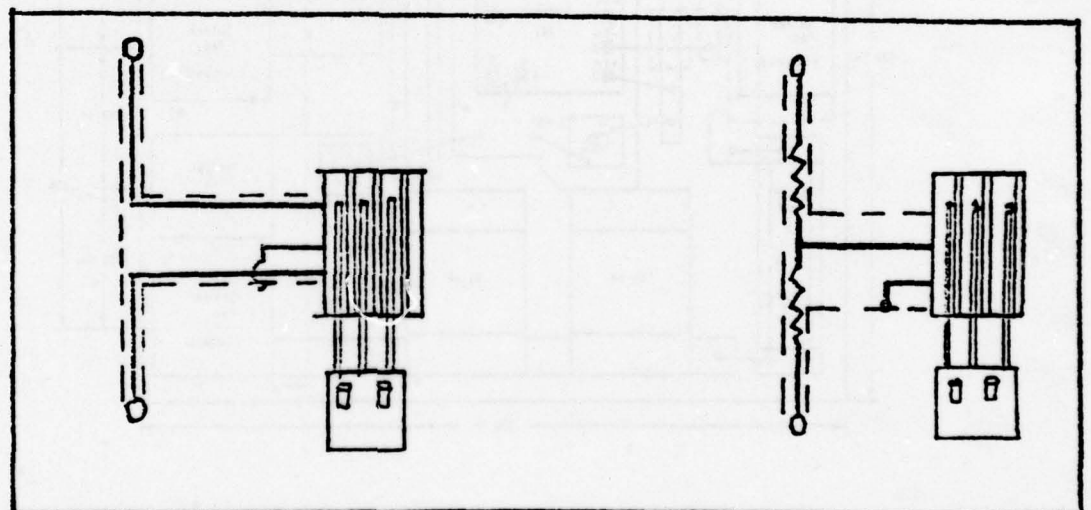
1. Resilient Adhesive in Bearing Preload Set Up in No. 3 Assembly.

2. All Bearings Glued On Both Inner And Outer Races, Except Units 1 and 2.





CONSTRUCTION DETAILS



SINGLE ENDED HOOKUP

DOUBLE ENDED HOOKUP

Figure 11. Electric Field Probe Design.

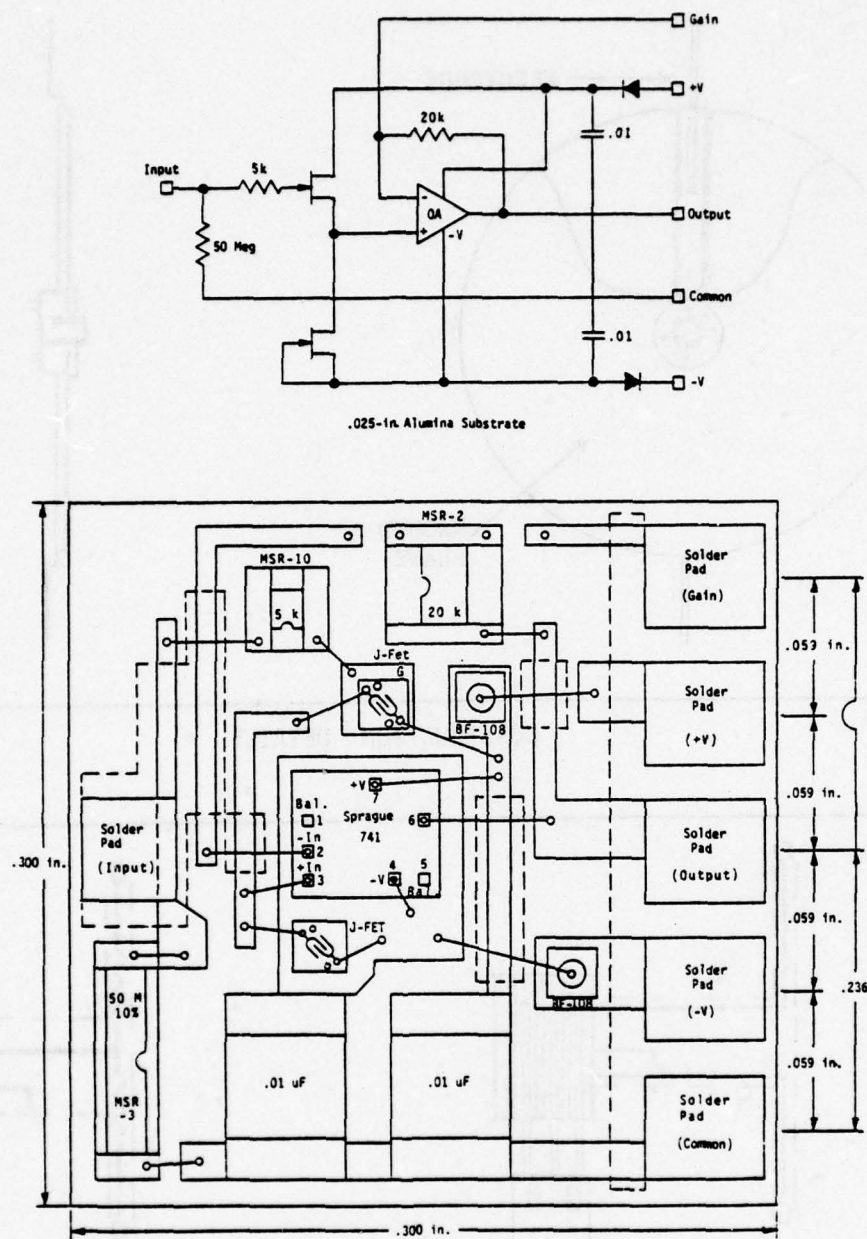
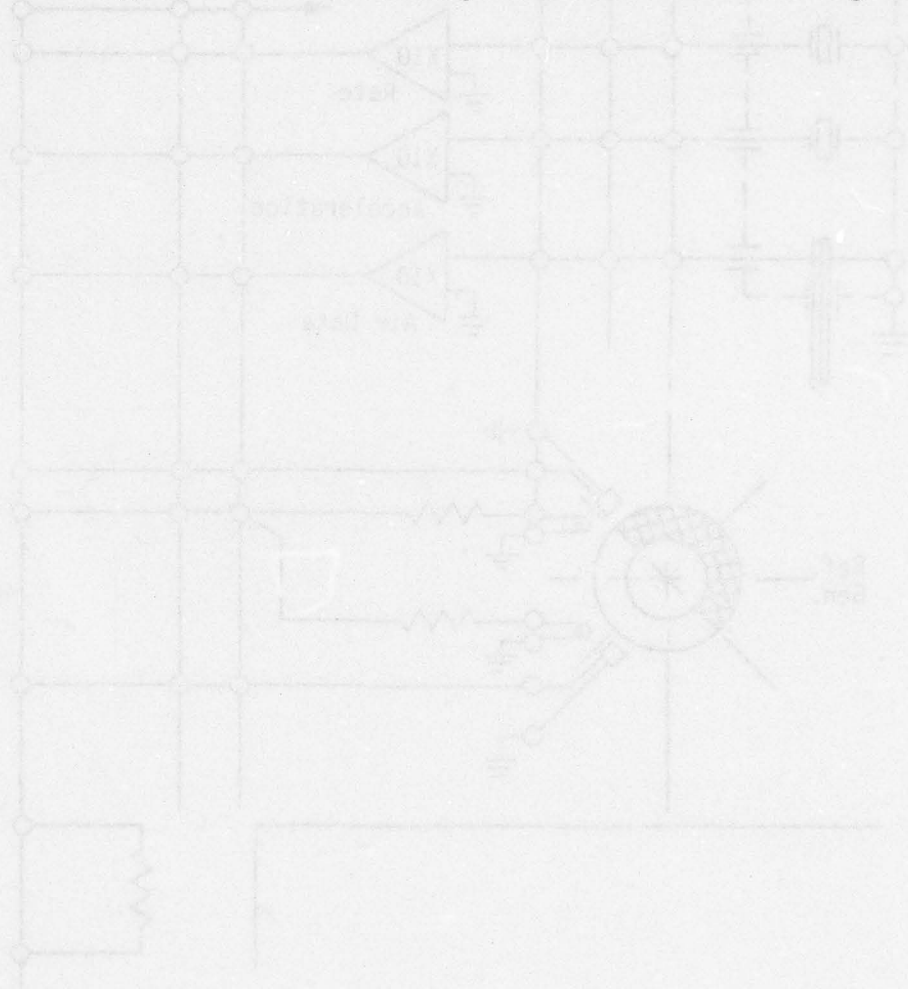


Figure 12. Isolation Preamplifier -Nonmagnetic Construction.

included are the temperature compensating capacitors bridging the crystal output across the isolation preamplifier input. This installation is supplied with top and bottom external shields to reduce the cross talk from the reference generator circuits. The isolation preamplifier is capable of an output in excess of 6 V r.m.s., with an adjustable gain of 1 to 100, an input impedance of 100 megohms, and an output impedance of 8 to 14 ohms.

The typical instrument hookup schematic is shown in Figure 13.





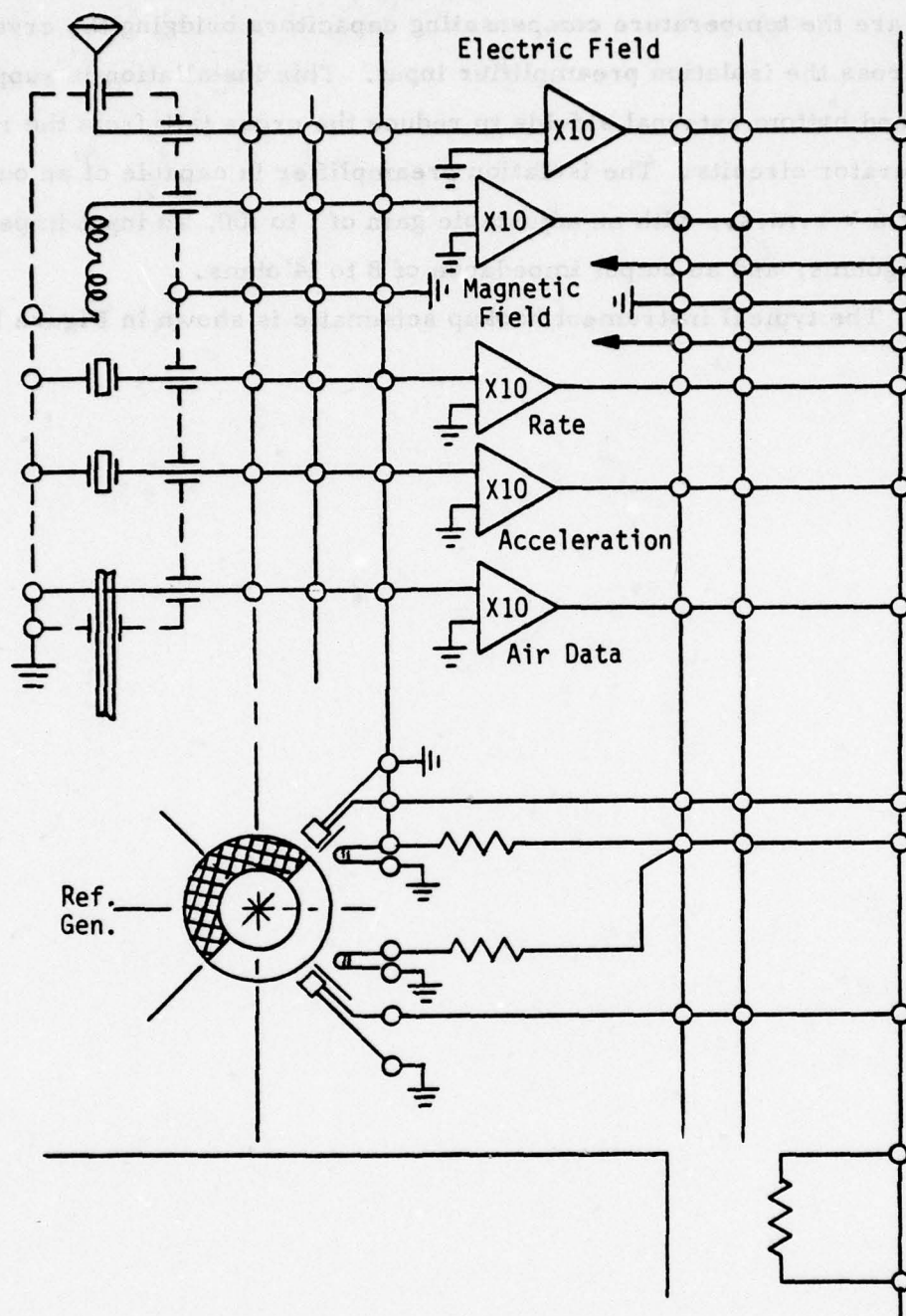


Figure 13. Multi-Sensor Internal Schematic.

## SECTION IV TEST AND EVALUATION

### 4.1 TEST SETUP DESCRIPTION

The various test arrangements for evaluating the nominal performance of the multi-sensor are described below.

#### REFERENCE TEST STAND (GENERAL)

The reference test stand was designed and built for this sensor development activity and is organized to set up and/or control the various input phenomena to be sensed. It supplies the "reference" inputs against which to measure the performance of the multi-sensor.

#### ANGULAR VELOCITY INPUT

To supply angular velocity inputs to the sensor, a rate table was employed with discrete settings covering the range of  $\pm 0.2^\circ/\text{sec.}$  to  $\pm 18^\circ/\text{sec.}$

#### LINEAR ACCELEROMETER INPUT

The performance of the linear accelerometer is determined by inputs to the earth's "g" field controlled by angular displacements via a precision tumbling table. This arrangement allows  $\pm 1.0$  "g" in increments as small as 0.005 "g".

#### X/Y/Z AXIS MAGNETIC FIELD INPUTS

The reference magnetic field is supplied by permanent magnets on the test stand arranged in such a way as to supply vertical and/or horizontal components approximating that of the earth's field. In conjunction with the tumbling table, this allows precise input increments.

#### ELECTRIC FIELD INPUT (OPEN TEST)

To measure the relative performance of the electrometer in a typical airborne installation, the sensor was mounted in a simulated missile shape, the whole of which was rotatable within the electric field, supplied by the reference test stand.

## AIR DATA INPUT

With the sensor mounted in the simulated missile shape, air flow input up to 100 m.p.h. was supplied by a variable speed blower attached to the reference test stand. Together with the ability to rotate the air shape within the reference test stand, this allowed angle of attack, as well as air speed measurements to be made with the multi-sensor.

The performance of the gas drive system, which includes the pressure regulator, filter and venturi source, is described in Table 3.

Table 3. Threshold and Speed Regulation  
Tests Using 9-in. Hg Venturi No. 2

Run at 130 m.p.h. Set Vacuum Regulator at 100 r.p.s. Then start at 50 m.p.h. and go in 10 m.p.h. increments to 130 m.p.h.

$u_T$ , m.p.h.	P, in. Hg	$f_s$ , Hz
130	2.50 speed	100
50	0.75	46
60	1.20	62
70	1.65	79
80	2.20	94
90	2.25 switching regulator	95
100	2.40	98
110	2.50	99
120	2.55	101
130	2.55	101

## 4.2 MULTI-SENSOR LABORATORY TESTS DESCRIPTIONS

### ANGULAR VELOCITY TEST

#### Setup No. 1

The sensor was arranged on the rate table with the spin axis perpendicular to the gravity field and with the rate table axis of rotation coupled into the sensitive axis of the device. The object of this particular test setup is to gather data on linearity, symmetry and scale factor.



## LINEAR ACCELERATION TEST

### Setup No. 2

The linear accelerometer portion of the instrument was tested with one axis aligned perpendicular to the "g" field. This allows the device to be operated essentially as a single-axis input.

## ACCELEROMETER RETEST

### Setup No. 2a

The accelerometer section was remeasured in a test configuration where the sensor is tumbled about the spin axis in the 1 "g" field. This test operates the device for two-axis function.

## X/Y MAGNETOMETER TEST

### Setup No. 3

The X/Y magnetometer was measured in the reference test stand with the spin axis vertical and with the input motion about the spin axis, causing a sine/cosine varying function to be applied to the resolved output axis. The parameters measured included scale factor and some linearity data.

## Z AXIS MAGNETOMETER TEST

### Setup No. 4

The initial test on the Z magnetometer revealed a scale factor approximately 100 times lower than desired. However, some functional tests and a determination of linearity for small angles were made. The important conclusion for the tests on the Z axis magnetometer probe showed that the signal information, although "low level," was very stable and had good null repeatability, thus allowing a reasonably optimistic prediction for its final outcome in a subsequent redesign. Of note is that this probe does not operate through a slip ring joint, and is not high impedance.

## X/Y ELECTROMETER TEST

### Setup No. 5

The electrometer probe was initially measured in an open-to-the electric field environment, unlike a typical missile or aircraft installation. The reason for making measurements in this fashion was to gather baseline performance data upon which to differentiate the effects of a typical installation on the sensor's scale factor and linearity. The measurements resulted in determining the scale factor and linearity for small angle inputs.

## X/Y ELECTRIC FIELD TEST (SPIN AXIS HORIZONTAL)

### Setup No. 6

This test series placed the sensor assembly in a simulated missile air shape in such an arrangement as to present the electric field and air data probes to the simulated electric field and air flow environment. Measurements on the electrometer similar to those made in Setup No. 5 were repeated and information was gathered related to linearity and scale factor, thereby allowing correlation of the effects of the presence of the body shape in the electric field close to the transducer.

## X/Y ELECTRIC FIELD TEST (SPIN AXIS VERTICAL)

### Setup No. 7

The air shape and sensor assembly was rotated around the sensor spin axis in the test fixture, to present the electric field sensor to the electric field reference source in a different fashion than that obtained in Setup No. 6. The field in Setup No. 6 lies parallel to the spin axis, and perpendicular in Setup No. 7. In the case of Setup No. 6 configuration, the reason for making discretely different measurements in this fashion was to determine the small angle accuracy for pitch and roll, similar to that of the operational environment where the electrometer would be used as a vertical reference, and would operate around null. With the spin axis perpendicular to the electric field, data was gathered with respect to scale factor variation due to large angle (90°) displacement.

## AIR DATA TEST

### Setup No. 8

Due to the scope and emphasis of the initial effort on this sensor feasibility development program, no gas flow source to simulate 0 to 250 m.p.h. airspeed was made. Instead a "local to the sensor flow" of 0 to 100 m.p.h. was used. Information was gathered as to the scale factor and small angle input measurements relating to null uncertainties. It was determined that the device functions to transduce the measurement of the input phenomenon as a simple inverse function. Small angle measurements were made to simulate the operation of the device as an angle of attack sensor. This was done with the airflow set at approximately 60 m.p.h. The angle of attack linearity was measured for angles up to  $\pm 20^\circ$ .

### NULL UNCERTAINTY TEST (SPIN AXIS HORIZONTAL)

#### Setup No. 9

The null uncertainty series was made with the sensor mounted rigidly to the granite leveling table in the test reference system with an electrostatic and magnetic shield surrounding the device. These measurements were made with most of the data extracted from strip chart recordings.

### NULL UNCERTAINTY TEST (SPIN AXIS VERTICAL)

#### Setup No. 10

This was identical to the preceding run except that the multi-sensor spin axis was mounted vertical to the "g" field. The parameters of interest in the null uncertainty test series included the noise band from dc up to the limits of the recording technique, which in this case was 60 Hz.

At this point in the evaluation of the sensor, sufficient data has been gathered on all the probes to specifically define the scale factors, and null uncertainties, but not the linearity and symmetry. Subsequently, the sensor is completely recycled through the test set in such a way as to allow the various inputs to be made to determine the cross quantity coupling coefficients. In the case of rate sensitivity, this is done by mounting the device in a rate input (test setup) and looking for unwanted rate response on the probes other than the rate detector.



#### 4.3 TEST RESULTS SUMMARY AND CONCLUSIONS ANGULAR VELOCITY PROBE

The angular velocity probe, because of its relative importance in most of the applications intended for such a device, is probably the most critical of those instrumented, particularly the null uncertainty.

The null uncertainty is tied to the specific design and execution of the dynamic alignment control of the spin axis, as well as the spin bearing smoothness.

The linear 'g' cross coupling in the rate section is primarily controlled by the specific alignment of the crystal probe in the build cycle and the spin velocity of the rotor. It is felt that refined assembly tooling should control the linear 'g' coupling to the number anticipated in the projected performance. The bias parameter is also related to the spin axis dynamic balance component and its thermo-mechanical stability.

The effects of spin velocity variations on the rate section occur in two major areas, one having to do with change of the null operating point or bias as a function of spin velocity, and the other with the change in scale factor as a function of spin velocity. With respect to the scale factor change, it is a normal function and no design fix other than control of the spin velocity is apparent. With respect to the change of bias as a function of the spin velocity, as the bias level is reduced, the bias uncertainty will drop commensurately.

#### LINEAR ACCELERATION PROBE

The major limitation on the accelerometer section has to do with the null uncertainty as a function of spin velocity variation.

The major conclusion is that when the rate performance is improved the accelerometer will benefit directly also. Unlike the rate probe, the linear acceleration scale factor does not change as a function of spin velocity, hence, design solutions other than spin speed control are possible.

## AIR DATA PROBE

The major problem with the air data probe has to do with the inability to apply precise inputs, that is, air flow control over a significant dynamic range, i.e., 10 to 400 m.p.h. This is an area requiring a proper flow source to support any further development effort.

## X/Y AXIS MAGNETIC PROBE

With respect to the X/Y magnetometer, no important anomaly was identified, but additional testing under temperature changes is required.

## Z AXIS MAGNETIC PROBE

The Z axis magnetometer was modified to improve the scale factor in three ways: the number of turns on the coil was increased; the spin velocity was increased from 6000 r.p.m. to 12,000 r.p.m., and the number of reluctance switches was increased from 2 to 4. When these were in effect, the scale factor was increased to a practical level.

## ELECTRIC PROBE

The electrometer section's most important problem was installation anomalies from the adjacent mounting surfaces. If the surface is gold plated 3 or 4 in. around the probe, performance is acceptable.

A summary of these initial development problems and corrections is shown in Table 4.

The results of tests on eight gas driven multi-sensors, with respect to the various probes against common performance parameters, are summarized and presented in composite form in Table 5.

A typical set of data for a single cycle bench evaluation for the multi-sensor is included in Appendix A.

TABLE 4. MULTI-SENSOR: H.O.G. NO. 2 PERFORMANCE PROBLEMS

<u>Problem</u>	<u>Correction</u>
X/Y RATE	
1. Dynamic null uncertainties	1. Fasten BRG'S using adhesive technique
2. Linear "g" coupling	2. Run at 12,000 r.p.m.
3. High bias	3. Increase inertia of rotor about spin axis
4. Speed sensitivity	4. Remove crystal drive masses
5. Linearity	5. Remove crystal parasitic capacitive loading
	6. Prove buffer amplifier isolation
X/Y ACCELERATION	
1. X/Y magnetic field coupling	1. Prove buffer amplifier isolation
2. Air mass flow coupling	2. All of rate section corrections on spin axis suspension
3. Angular velocity coupling	3. Optical dividing head for inputs
4. Linearity	
X/Y ELECTROMETER	
1. High bias	1. Prove buffer amplifier isolation
2. X/Y magnetic field coupling	2. Carrier filtering
3. Angular velocity coupling	3. More closely simulate reference environment typical installation
4. Linear acceleration coupling	
X/Y MAGNETOMETER	
1. Linearity	1. More testing to establish reference quality ambient noise
Z MAGNETOMETER	
1. Low scale factor	1. 3 to 5 times more turns on coil
2. Linearity	2. 12,000 r.p.m.
	3. Carrier filtering



TABLE 4. MULTI-SENSOR: H.O.G. NO. 2  
PERFORMANCE PROBLEMS - CONTINUED

<u>Problem</u>	<u>Correction</u>
X/Y AIR DATA	
1. Linearity	1. Prove buffer amplifier isolation
2. X/Y magnetic field cross coupling	2. Carrier filtering
3. Linear "g" cross coupling	3. Better test setup (simulating installation)

TABLE 5. MULTI-SENSOR PERFORMANCE SUMMARY

No.	Parameters	I X/Y Axis Magnetic Field	II Z Axis Magnetic Field	III X/Y Axis Electric Field	IV Air Speed	V Air Flow	VI Angular Velocity	VII Linear Acceleration
1.	Signal Amplification	<x250.	<x50,000.	<x10,000.	<x50.	<x50.	<x10.	<x20.
2.	Carrier Filter	No	Yes	Yes	Yes	Yes	Yes	Yes
3.	Demod. Filter	Yes	Yes	Yes	Yes	Yes	Yes	Yes
4.	Response to Step Input	< .1 s	< .1 s	< .1 s	< .01 s	< .01 s	< .01 s	< .01 s
5.	Scale Factor (V d.c.)	5. V/G	5. V/G	.017 V/M	.010 V/ mi/h	.165 V/ <sup>0</sup>	.017 V/ <sup>0</sup> /s	.250 V/"g"
6.	Bias (Total Vector)	< .002 G	< .01 G	< 3. V/M	< 2. mi/h	< .5 <sup>0</sup>	< .02 <sup>0</sup> /s	< .002 "g"
7.	Threshold	< .0001 G	< .0001 G	< .3 V/M	< .2 mi/h	< .05 <sup>0</sup>	< .001 <sup>0</sup> /s	< .0003 "g"
8.	Null Uncertainty (Dynamic)	< .005 G p-p	< .001 G p-p	< 1. V/m p-p	< 2. mi/h p-p	< 1.0 <sup>0</sup> p-p	< .01 <sup>0</sup> /s p-p	< .001 "g" p-p
9.	Null Uncertainty (h to h)	< .0005 G rms	< .0005 G rms	< .5 V/m rms	< .3 mi/h rms	< .1 <sup>0</sup> rms	< .003 <sup>0</sup> /s rms	< .0005 "g" rms
10.	Null Uncertainty (Turn-On to Turn-Off)	< .0008 G p-p	< .0005 G p-p	< 1. V/m p-p	< .5 mi/h p-p	< .25 <sup>0</sup> p-p	< .008 <sup>0</sup> /s p-p	< .0008 "g" p-p
11.	Null Uncert. (Velocity Variation $\pm$ 10%)	< .001 G p-p	< .0005 G p-p	< 1. V/m p-p	< 2. mi/h p-p	< .30 <sup>0</sup> p-p	< .01 <sup>0</sup> /s p-p	< .002 "g" p-p
12.	Linear Operating Range	1.0 G	1.0 G	300. V/m	500. mi/h	$\pm$ 30. <sup>0</sup>	300 <sup>0</sup> /s	20 "g"
13.	Max. Overrange Input	5.0 G	5.0 G	1000. V/m	1000. mi/h	$\pm$ 180 <sup>0</sup>	1200 <sup>0</sup> /s	100 "g"
14.	Linearity (% Deviation from Nominal Scale Factor)	< 1.%	< 1.%	< 2.%	< 2.%	< 1.5%	< 1.%	< .5%
15.	Symmetry (Slope Agreement)	< 1.%	< 1.%	< 2.%	----	< 1.5%	< 1.%	< .5%

TABLE 5. MULTI-SENSOR PERFORMANCE SUMMARY - CONTINUED

No.	Parameters	I X/Y Axis Magnetic Field	II Z Axis Magnetic Field	III A/Y Axis Electric Field	IV Air Speed	V Air Flow	VI Angular Velocity	VII Linear Acceleration
16.	Cross Axis Coupling	< 2.%	---	< 2.%	By the Cos of Air Flow	By the Amplitude of Air Speed	< 2.%	< .5%
17.	Cross Quantity Alignment	< ± .5°	< ± .5°	< ± .5°	< ± .5°	< ± .5°	< ± .25°	0° (Ref.)
18.	Cross Quantity Coupling							
	I. X/Y Axis Mag. Field	100%	---	Negligible	Negligible	Negligible	Negligible	Negligible
	II. Z Axis Mag. Field	---	100%	Negligible	Negligible	Negligible	Negligible	Negligible
	III. X/Y Axis Elec. Field	Negligible	Negligible	100%	Negligible	Negligible	Negligible	Negligible
	IV. Air Speed	Negligible	Negligible	< .001 V/m/ m/h	100%	-----	Negligible	Negligible
	V. Angle of Air Flow	Negligible	Negligible	Negligible	-----	100%	Negligible	Negligible
	VI. X/Y Axis Ang. Velocity	Negligible	Negligible	Negligible	Negligible	Negligible	100%	100%
	VII. X/Y Axis Lin. Accel.	Negligible	Negligible	Negligible	< .02 m/h/ h/ "g"	< .05 o/ "g"	< .0002 o/ s/"g"	< .00005 "g"/ o/s
19.	Cross Quantity Coupling Compensation Factor	None	None	For Air Speed ± 10	For Linear Acceleration ± 10	For Linear Acceleration ± 10	For Linear Acceleration ± 100	For Angular Velocity ± 100



# SECTION V

## PROTOTYPE GAS DRIVEN MULTI-SENSOR DESIGN

### AND PROJECTED COST DATA

Figures 14, 15 and 16 depict a design of the gas driven multi-sensor in which extensive molded plastic fabrication techniques were used. This design was reached in collaboration with a specialist molding fabricator and tooling design house. It maintains a close thermo-mechanical and structural similarity to the previous evaluation units, which were fabricated out of machine parts. The molding material selected is a glass reinforced phenolic compound (see Table 6). Estimates of the cost of the multi-sensor using the molding approach are described in Tables 7 through 10.

The electronics signaling condition module, which is referred to in Figure 17 was developed by Natel Engineering. Each channel performs to the specification outline shown in Table 11.

The module is arranged on PC boards, four channels per board, such that the various output combinations and the options of the multi-sensor can be supported without any changes to the PC mother board.

Both gain and null offset adjustments are provided. The gain is to enable the output to be adjusted exactly.

Three reference amplifiers are supplied, one for the 200-Hz, 0° phase, one for the 200-Hz, 90° phase, and one for the 800-Hz, 0° phase. Each amplifier can provide the reference drive for six demodulators.

The configurations have all the potentiometer adjustments located at the edge of the board, at the opposite end from the connector, and they are labeled by channel. Forty-two connections are required with all input and reference signals being isolated (transformer coupled).

The following chart summarizes the cost based on variations of filter configuration and the number of adjustments brought out.

QTY	D510-5-J-XX-3 3-pole filter w/o adj.	D510-5-J-XX-3-AN 3-pole filter with adj.	D510-5-J-XX-2 2-pole filter w/o adj.	D510-5-J-XX-2-AN 2-pole filter with adj.
100	\$717(\$65/chan)	\$792(\$72/chan)	\$605(\$55/chan)	\$682(\$62/chan)

The projected cost of the signal conditioning modules in quantities of a thousand at rates of 100 per month or more would be no more than \$25 per channel.

Based on the cost analysis summarized in this data, a reasonably realistic tradeoff comparison can be made for a strapdown heading and attitude reference and stability system. This comparison is summarized in Figure 18 for complexity and in Figure 19 for cost.

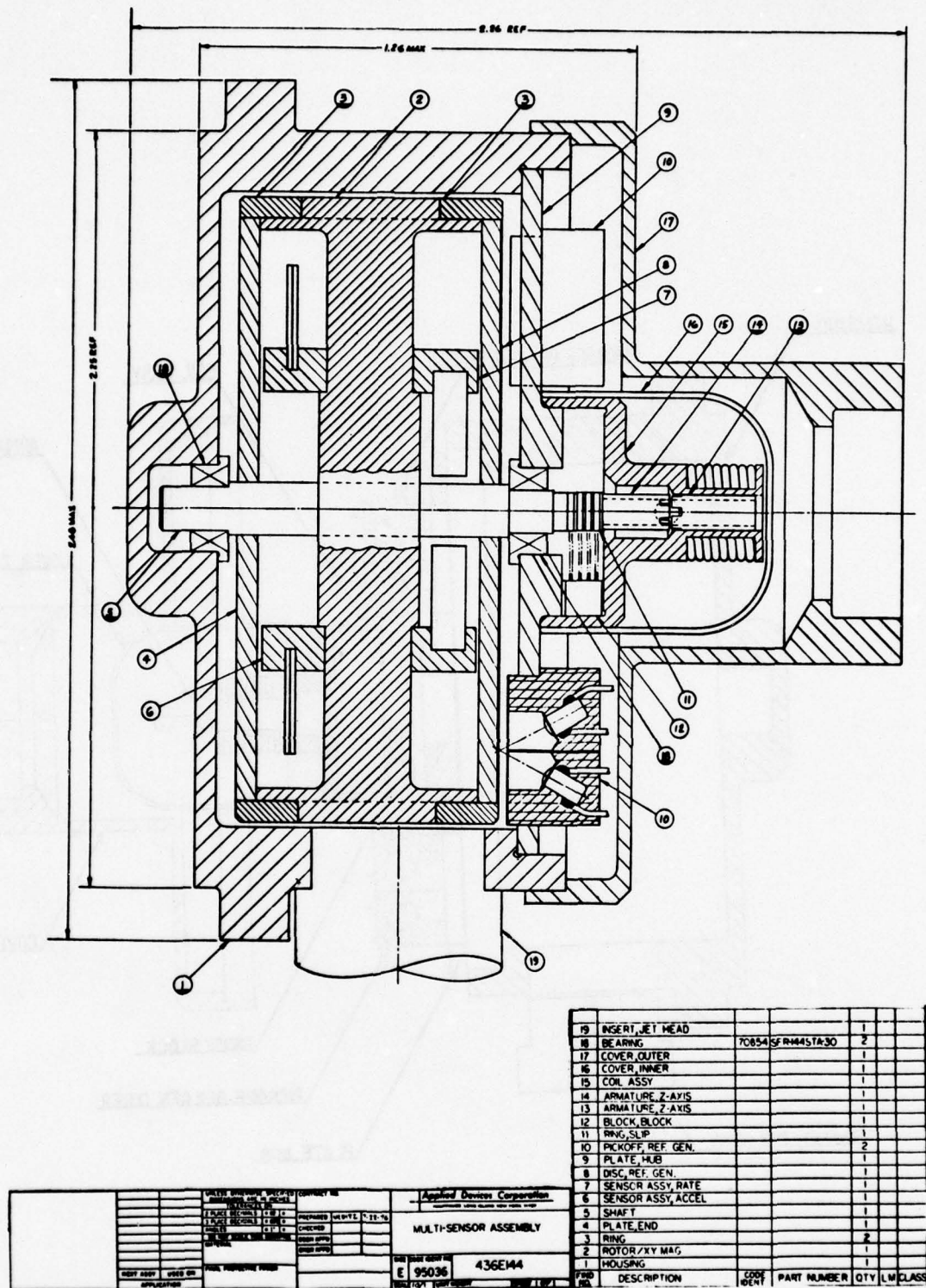


Figure 14. Prototype Multi-Function Sensor (Gas Driven).



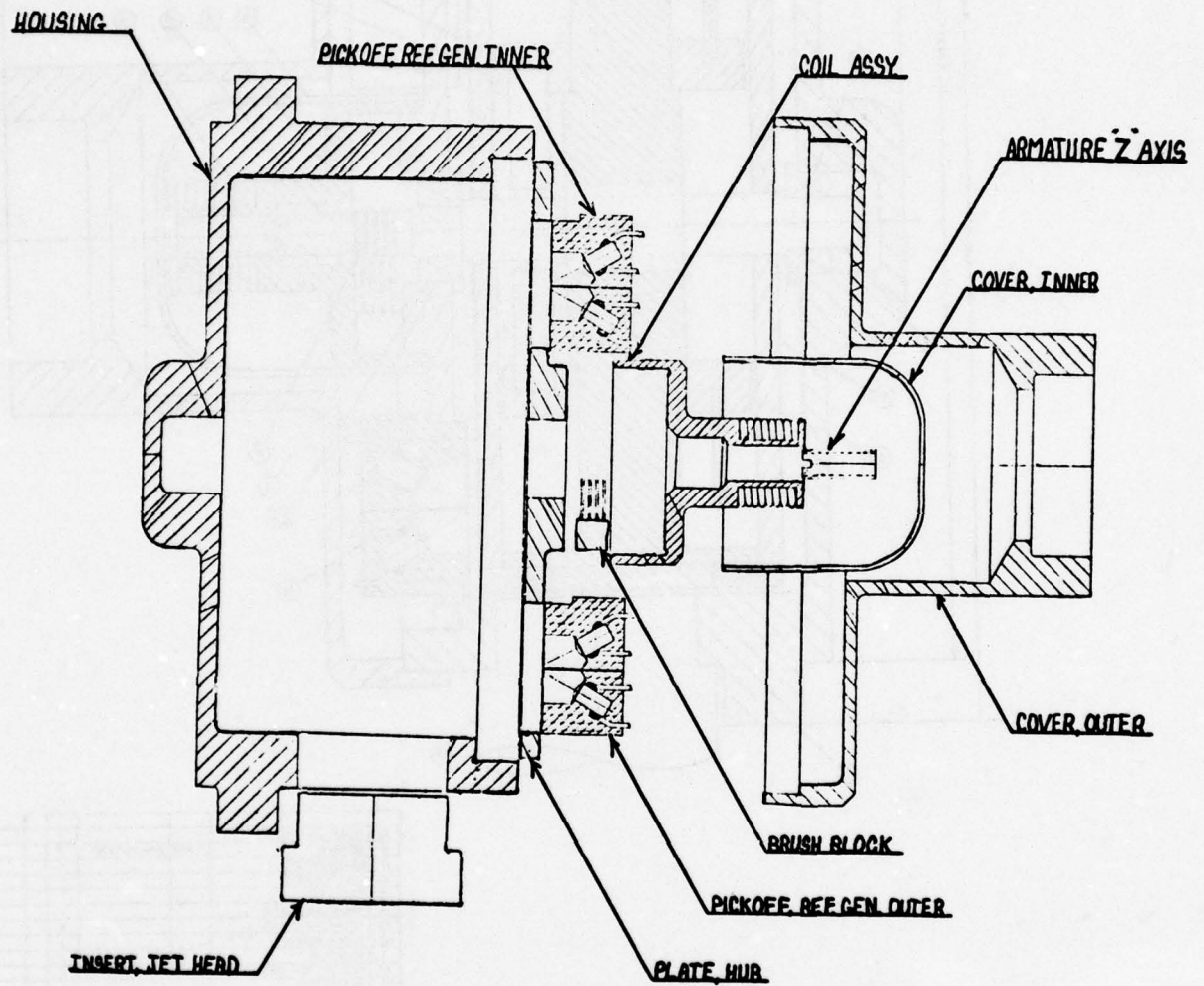


Figure 15. Multi-Sensor Housing Assembly Molded Configuration.

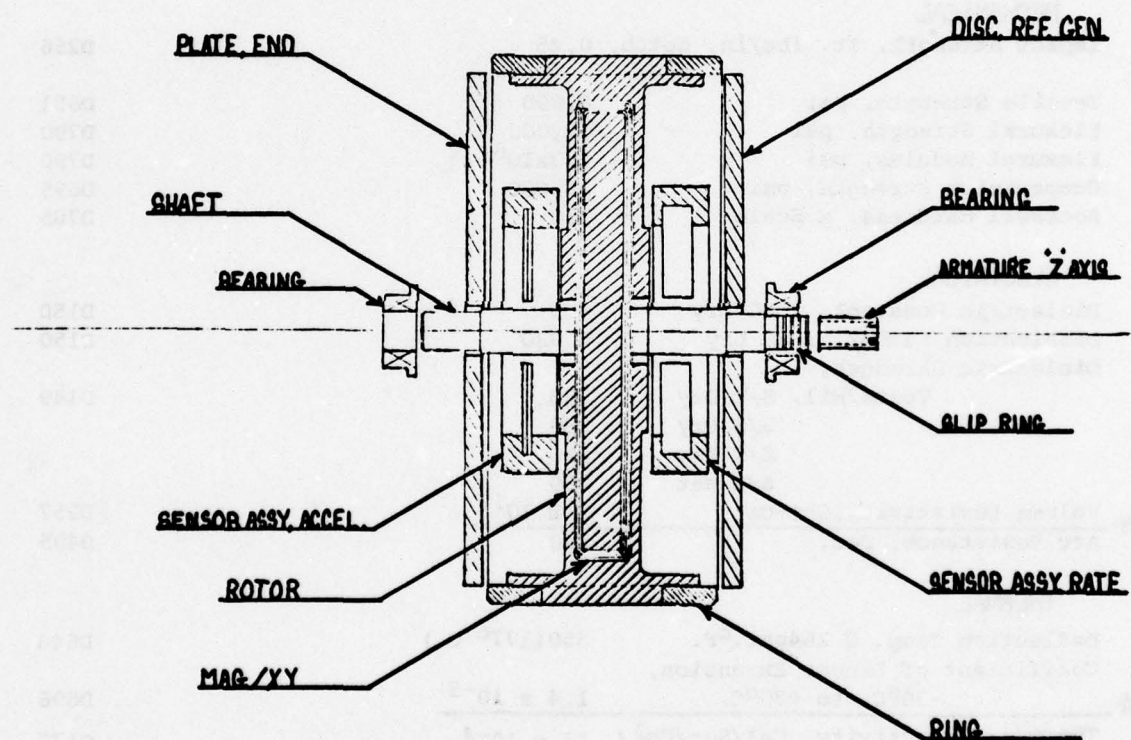


Figure 16. Multi-Sensor Rotor Assembly Molded Configuration.

TABLE 6. MULTI-FUNCTION SENSOR MOLDING MATERIAL FIBERITE 4004

COMPOUND PROPERTIES	AVERAGE VALUE	ASTM TEST METHOD
Form	Granular	
Color	Green, Black	
Bulk Factor	2.5-3.5	D954
* Molding Pressure, psi, Transfer	1,000-3,000	
* Compression	1,000-2,000	
* Plasticity	Medium-Soft(Spiral Flow Control)	
* Molding Temperature, °F	290-350	D957
PROPERTIES OF MOLDED SPECIMENS		
PERMANENCE		
Specific Gravity	1.90-1.95	D792
* Molding Shrinkage in./in.	0.0015-0.0030	D955
* Water Absorption, %, 24 Hrs @ 23° C.	0.10	D570
48 Hrs @ 50° C.	0.15	
MECHANICAL		
Impact Strength, ft. lbs/in. notch, side	0.45	D256
Tensile Strength, psi	8,000	D651
Flexural Strength, psi	12,000	D790
Flexural Modulus, psi	2.3x10 <sup>6</sup>	D790
Compressive Strength, psi	38,000	D695
Rockwell Hardness, M Scale	110	D785
ELECTRICAL		
Dielectric Constant, 1 MC Dry	4.5	D150
Dissipation Factor, 1 MC Dry	0.020	D150
Dielectric Strength, Volts/Mil, S/T Dry	320	D149
S/S Dry	280	
S/T Wet	320	
S/S Wet	280	
* Volume Resistivity, Ohm-cm	2 x 10 <sup>13</sup>	D257
* Arc Resistance, Sec.	180	D495
THERMAL		
Deflection Temp. @ 264psi, °F.	350(177° C.)	D648
Coefficient of Linear Expansion, -30°C. to +30°C.	1.4 x 10 <sup>-5</sup>	D696
* Thermal Conductivity, Cal/Sec/Cm <sup>2</sup> /°C/Cm	13 x 10 <sup>-4</sup>	C177

Fiberite 4004 is a glass reinforced two-stage phenolic molding compound. This low bulk granular material is ideally suited for automatic preforming. The material is characterized by long flow, low molded shrinkage, excellent dimensional stability. Recommended to molders desiring approval under Type MFH of Military Specification Mil-M-14F.



TABLE 7. MULTI-MODE SENSOR COMPRESSION/TRANSFER  
MOLDING TOOLING ESTIMATES

COMPRESSION/TRANSFER MOLDING TOOLING ESTIMATES			
<u>TOOL FAMILIES</u>			
I.	COVER	436C157	
	ROTOR HOUSING RING	436D146	
	END PLATE (REF.)	436C148	\$10,170.00
	HUB PLATE, W/Mtg	436C153	
	Provisions for LEDs		
II.	BOBBIN COVER	436D155	
	HOLDER, RATE	436C151	
	HOLDER, ACCEL.	436C150	\$ 5,500.00
	JET HEAD	436C118	
III.	ROTOR INSERT	436D146A	\$ 3,500.00
IV.	ROTOR BODY	436D146B	\$ 4,625.00
TOTAL			\$23,795.00

TABLE 8. MULTI-MODE SENSOR MOLDED PARTS COST PROJECTIONS

BUDGETARY			QUANTITIES	
			50	1000
I.	COVER	436C157	3.02	.39
	ROTOR HOUSING RING	436D146	5.45	.45
	END PLATE (H/S)	436C148	4.95	.65
	HUB PLATE	436C153	4.75	.35
II.	BOBBIN COVER	436D155	4.79	.29
	HOLDER, SENDER RATE	436C151	5.20	.25
	HOLDER, SENDER ACCEL	436C150	5.20	.25
	JET HEAD	436C118	4.75	.35
III.	ROTOR INSERT	436D146, A	5.15	.80
IV.	ROTOR	436D146, B	4.75	.74
TOTALS PER SET			\$48.01	\$4.52

TABLE 9. MULTI-MODE SENSOR OVERALL TOOLING COST PROJECTIONS

OVERALL TOOLING COST PROJECTIONS		
ITEM	SENSOR QUANTITIES	
	50/100	1,000/3,000
1. MOLDED PARTS	<u>24,000.00</u> +++++	
2. BRUSH BLOCK & SLIPRING	350.00	2,086.00
3. SPIN AXIS BEARINGS	NONE	1,000.00
4. REFERENCE GENERATOR	500.00	2,000.00
5. ISOLATION AMPLIFIERS	1,800.00	5,000.00
6. CONNECTOR/MOTHER BOARD	250.00	500.00
7. FINAL ASSEMBLY JIGS & FIXTURES	2,500.00	8,000.00
8. TEST SETS	1,500.00	6,000.00
<hr/>		
<u>TOTALS:</u>	\$31,000.00	\$25,600.00
<hr/>		
<u>RATE (APPROX.):</u>	15/Month	100/Month



TABLE 10. MULTI-MODE SENSOR COST PROJECTIONS (BARE COSTS)

COST PROJECTIONS (BARE COSTS)			
ITEM		SENSOR QUANTITIES	
		50/100	1,000/3,000
1.	MOLDED PARTS (PER SENSOR)	48.00	5.00
2.	BRUSH BLOCK & SLIPRING	39.00	28.00
3.	SPIN AXIS BEARINGS (PER SENSOR)	13.00	11.00
4.	REFERENCE GENERATOR PICKOFFS (2/SENSOR)	25.00	10.00
5.	ISOLATION AMPLIFIERS (2/SENSOR)	70.00	25.00
6.	CONNECTOR/MOTHER BOARD	10.00	4.00
MATERIAL TOTAL:		205.00	73.00
LABOR (@ 15.00/Hr.)		X12=180.00	X5=75.00
GRAND TOTAL:		<\$385.00	<\$148.00
(PER SENSOR)			

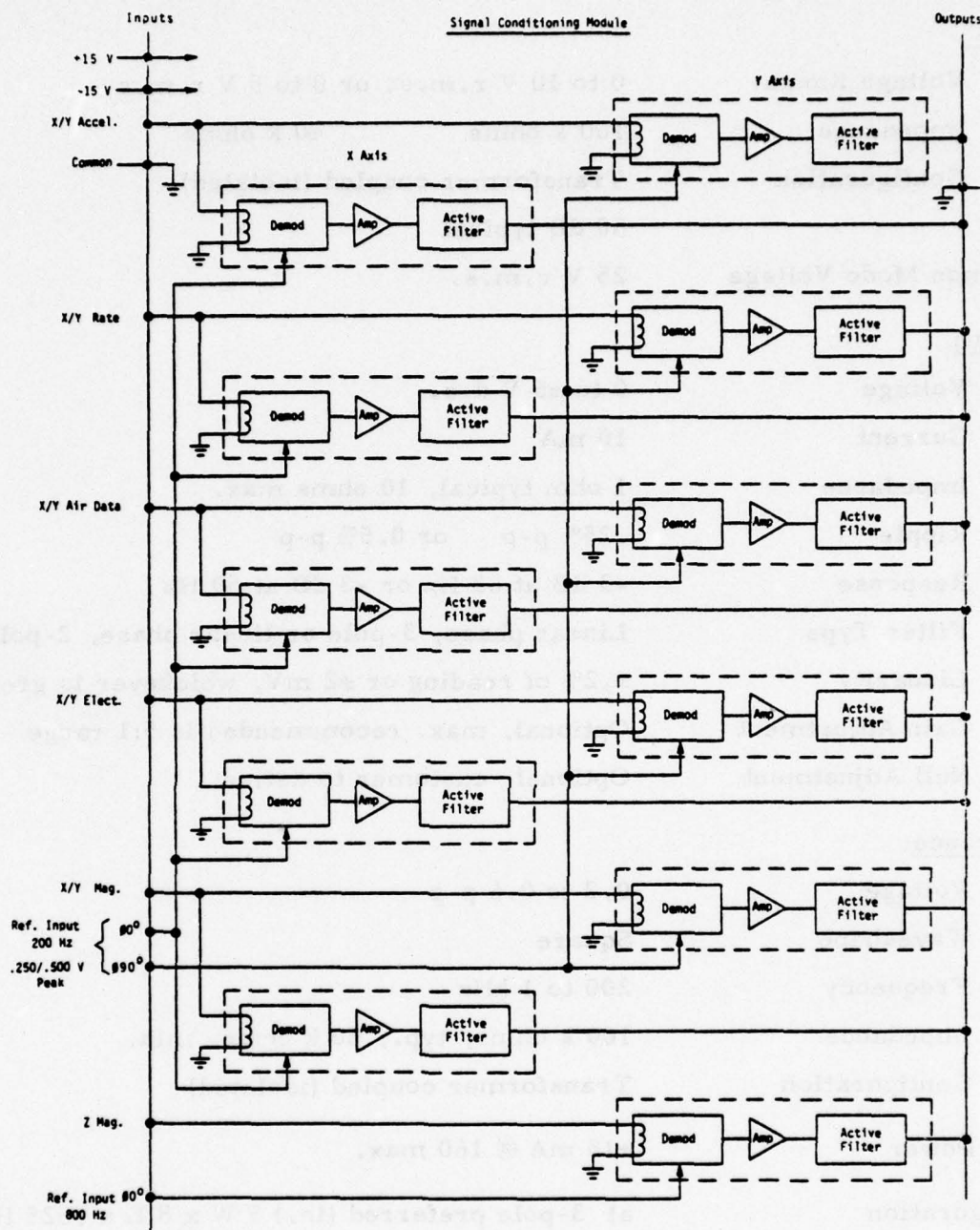


Figure 17. Multi-Sensor Signal Conditioning Module Schematic.

TABLE 11. SIGNAL CONDITIONING MODULE SCHEMATIC OUTLINE

Input

Voltage Range	0 to 10 V r.m.s. or 0 to 5 V r.m.s.
Impedance	100 k ohms                      40 k ohms
Configuration	Transformer coupled (isolated)
CMR	60 dB typical
Common Mode Voltage	25 V r.m.s.

Output:

Voltage	0 to $\pm 5$ V d.c.
Current	10 mA
Impedance	1 ohm typical, 10 ohms max.
Ripple	.25% p-p    or 0.5% p-p
Response	-3 dB at 63 Hz or -3 dB at 50 Hz
Filter Type	Linear phase, 3-pole or linear phase, 2-pole
Linearity	$\pm .2\%$ of reading or $\pm 2$ mV, whichever is greater
Gain Adjustment	Optional, max. recommended is 5:1 range
Null Adjustment	Optional, customer to define

Reference:

Voltage	0.2 to 0.6 p-p
Waveshape	Square
Frequency	200 to 1 kHz
Impedance	100 k ohms, typ., 50 k ohms, min.
Configuration	Transformer coupled (isolated)

D.c. Power                       $\pm 15$  mA @ 160 max.

Configuration                      a) 3-pole preferred (in.) 5 W x 8 L x .625 H  
    Minimum (in.)                      5 W x 6.5 L x .625 H  
    b) 2-pole preferred (in.) 5 W x 6 L x .625 H  
    Minimum (in.)                      5 W x 5 L x .625 H

Connector                              P.C. type, Dual 22 pin (44 connections)



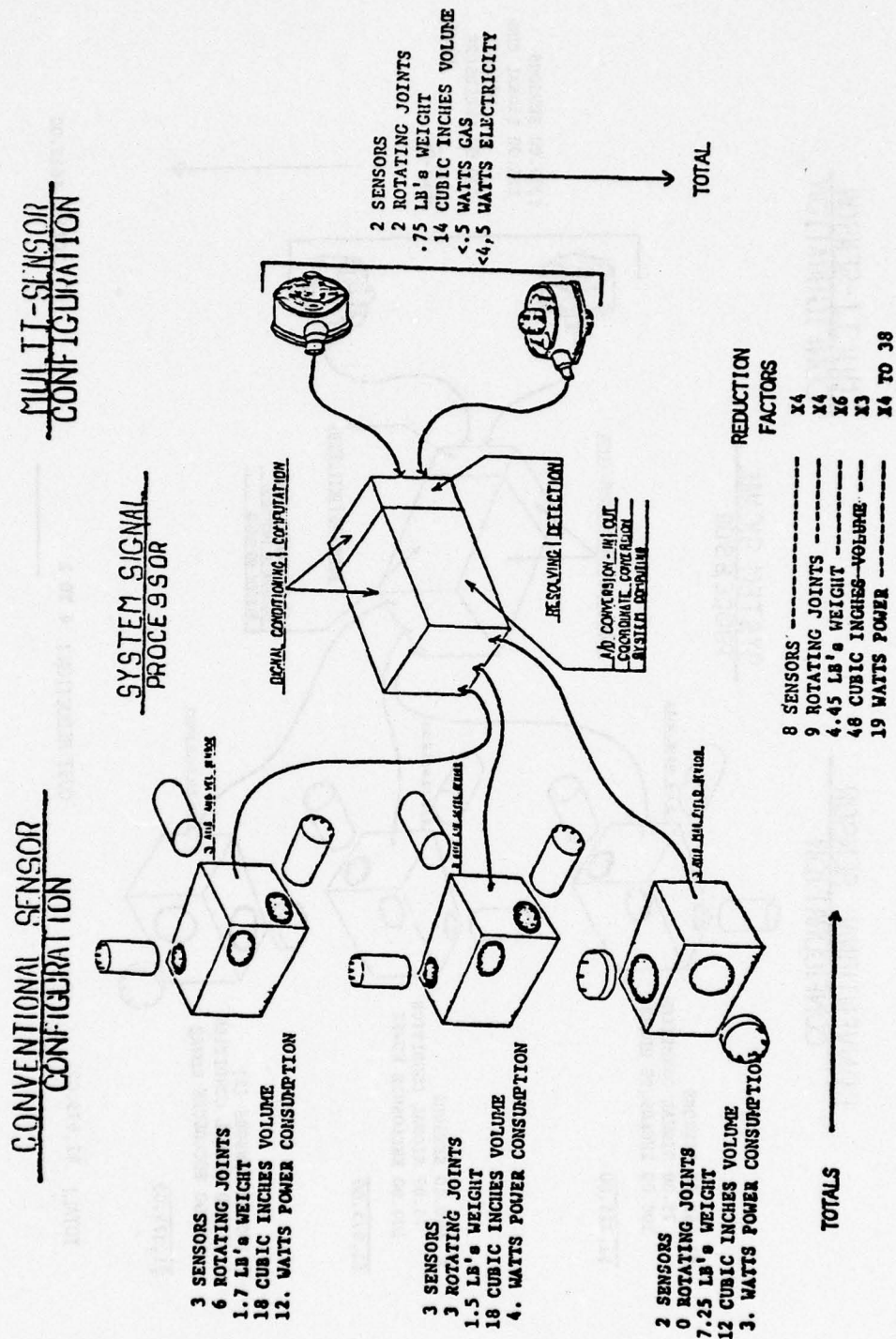
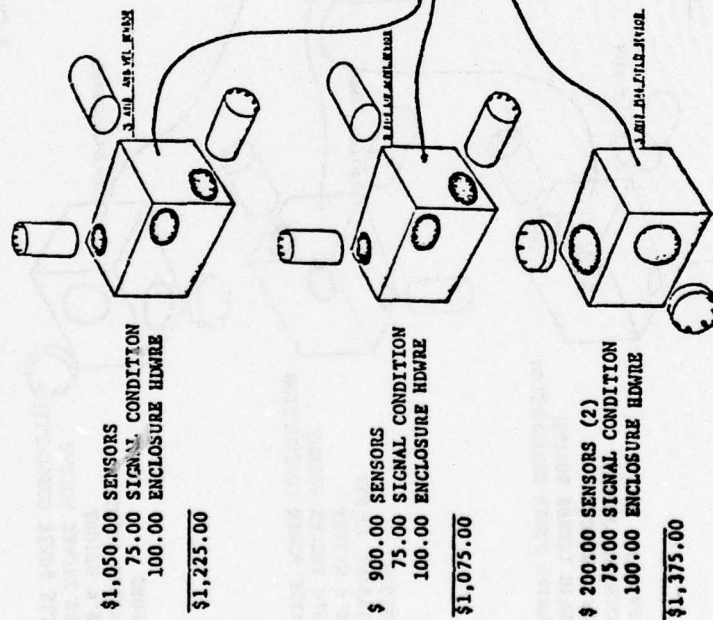


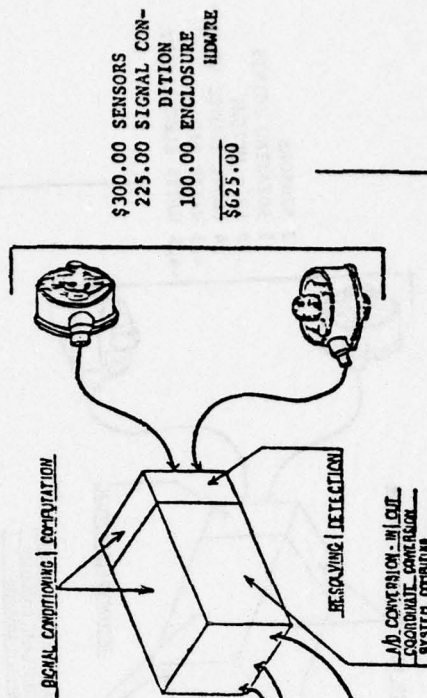
Figure 18. Strapdown, All Attitude, Heading and Attitude Reference System Comparison (Cost).

# CONVENTIONAL SENSOR CONFIGURATION



# MULTI-SENSOR CONFIGURATION

## SYSTEM SIGNAL PROCESSOR



TOTAL: \$2,675.00

COST REDUCTION: 4 TO 1

TOTAL: \$625.00

Figure 19. Strapdown, All Attitude, Heading and Attitude Reference System Comparison (Complexity).

## SECTION VI

### CONCLUSIONS AND RECOMMENDATIONS

Feasibility was clearly demonstrated for an ultra low cost multifunction sensor for flight control applications. This multifunction sensor, with only one moving part, performs the equivalent to a two-axis rate gyro, two-axis linear accelerometer, a three-axis magnetic field sensor, a two-axis electric field sensor, and a two-axis air data probe.

To exploit the potential of this multi-function sensing concept, it is recommended that additional work be done to define the performance characteristics under the using environment, including temperature vibration and shock. In addition, it is recommended that a group of instruments be built and evaluated under actual flight test conditions.



Appendix A

MULTI-SENSOR SUMMARY TEST RESULTS

TABLE A-1. MULTI-SENSOR SUMMARY TEST RESULTS

<u>Unit No.</u>	<u>Sensing</u>	<u>In Axis</u>	<u>Measuring Parameter</u>	<u>Value Obtained</u>	<u>Design Goal</u>	<u>Variances</u>
H.O.G.2 Run 1	Rate	X/Y	Linearity	<1.2%	<1.0%	>0.2%
H.O.G.2 Run 2	Linear Acceleration	X/Y	Linearity	<1.32%	<0.5%	>0.8%
H.O.G.2 Run 3	Linear Acceleration	X/Y	Linearity	<1.45%	<0.5%	>0.95%
H.O.G.2 Run 4	Magnetic Field	X/Y	Linearity	<7.5%	<2.0%	>5.5%
H.O.G.2 Run 5	Magnetic Field	Z	Linearity	<12.4%	<2.0%	>10.0%
H.O.G.2 Run 6	Magnetic Field	X/Y	Linearity	<1.7%	<2.0%	<0.3%
H.O.G.2 Run 7	Electric Field	X/Y	Linearity	<4.5%	<2.0%	>2.5%
H.O.G.2 Run 8	Electric Field	X/Y	Linearity	<1.9%	<2.0%	<0.1%
H.O.G.2 Run 9	Electric Field	X/Y	Linearity	<7.0%	<2.0%	>5.0%
H.O.G.2 Run 10	Air Data	X	Linearity	<4.0%	<2.0%	>2.0%
H.O.G.2 Run 11	Air Data	Y	Linearity	<2.0%	<2.0%	0
H.O.G.2 Run 12	Magnetic Field	X/Y	Null Uncert.	< $\pm 0.0003$ Gauss	< $\pm 0.0005$ Gauss	<0.0002 Gauss
H.O.G.2 Run 12	Air Data	X	Null Uncert.	< $\pm 2.3$ m.p.h.	< $\pm 1.5$ m.p.h.	>0.8 m.p.h.
H.O.G.2 Run 12	Air Data	Y	Null Uncert.	< $\pm 0.45$ deg.	None	-

TABLE A-1. MULTI-SENSOR SUMMARY TEST RESULTS - CONTINUED

<u>Unit No.</u>	<u>Sensing</u>	<u>In Axis</u>	<u>Measuring Parameter</u>	<u>Value Obtained</u>	<u>Design Goal</u>	<u>Variance</u>
H.O.G.2 Run 13	Rate	X/Y	Null Uncert.	$\leq \pm 0.03$ deg./sec.	$\leq \pm 0.002$ deg./ sec.	$> 0.28$ deg./ sec.
H.O.G.2 Run 13	Linear Acceleration	X/Y	Null Uncert.	$\leq \pm 0.002$ "g"	$\leq \pm 0.002$ "g"	$> 0.001$ "g"
H.O.G.2 Run 14	Electric Field	X/Y	Null Uncert.	$\leq \pm 3.0$ V/m	$\leq \pm 0.5$ V/m	$> 2.5$ V/m
H.O.G.3 Run 15	Air Data	X	Cross Axis Coupling	$< 8.0$ deg.	$< 1.0$ deg.	$> 7.0$ deg.
H.O.G.3 Run 16	Rate	X	Linearity	$\leq \pm 0.028$ deg./ sec.	$\leq \pm 0.002$ deg./ sec.	$< 0.026$ deg./ sec.
H.O.G.3 Run 17	Rate	Y	Linearity	$< 0.05$ deg./ sec.	$\leq \pm 0.002$ deg./ sec.	$< 0.048$ deg./ sec.
H.O.G.3 Run 18	Magnetic Field	X/Y	Tracking Accuracy	$\leq \pm 0.13$ deg.	$\leq \pm 0.3$ deg.	$< 0.17$ deg.
Elec. Driven Unit No.2 Run 19	Magnetic Field	X/Y	Tracking Accuracy	$\leq \pm 0.35$ deg.	$\leq \pm 0.3$ deg.	$> 0.05$ deg.
Elec. Driven Unit No.2 Run 20	Magnetic Field	X/Y	Motor Inter- action	$\leq \pm 0.45$ deg.	$\leq \pm 0.3$ deg.	$> 0.15$ deg.
H.O.G.5 Run 21	Electric Field	X/Y	Detecting Distant Moving Aircraft	$\approx 7500.0$ ft.	—	—

## Appendix B

### ELECTRICALLY DRIVEN MULTI-SENSOR DEVELOPMENT

#### B. 1 GENERAL

To give the multi-sensor a wider system applicability over the gas driven configuration, a need exists for an electric spin axis drive. Efforts were expended to establish the performance that could be achieved in the X/Y and Z axes magnetometer probes when the instrument is driven with a hysteresis synchronous motor. One of the most versatile combinations of the multi-sensor is one that includes angular velocity, linear acceleration, and magnetic field sensing (see Figures B-1 and B-2).

#### B.2 FEASIBILITY OF CO-FUNCTIONING OF THE MAGNETOMETER PROBE WITH AN ELECTRO-MAGNETIC SPIN AXIS DRIVE MOTOR

##### ROTATING COIL PROBE

Referring to Figure B-3, the most fundamental and persistent problem in a sensitive magnetic sensor working near any magnetic drive, using an induction motor, is the distortion of the field to be measured. The effect is one where the soft iron magnetic field conductive motor stator iron acts as a flux pipe to distort the ambient field that the rotating magnetometer probe coil is sensing.

Due to the symmetrical nature of the axis of rotation of the probe coil, with respect to the axis of symmetry of the motor stator, the effect is reduced.

In addition, due to the fact that the motor rotor, which is rotating with the probe coil, is magnetically hard and forms an enclosure for the soft iron of the stator, there is further reduction of the inductive effect.

Referring to Figure B-4, the effect of the motor excitation magnetic field leakage which becomes coherent when the rotor is in synchronism is reduced by a four-pole design which runs synchronus at  $1/2$  excitation frequency. Although this arrangement tends to reduce the noise at the fundamental frequency, there is some leakage, and hence coupling in the phase detection.



THIS PAGE IS BEST QUALITY PRACTICABLE  
FROM COPY FURNISHED TO DDG

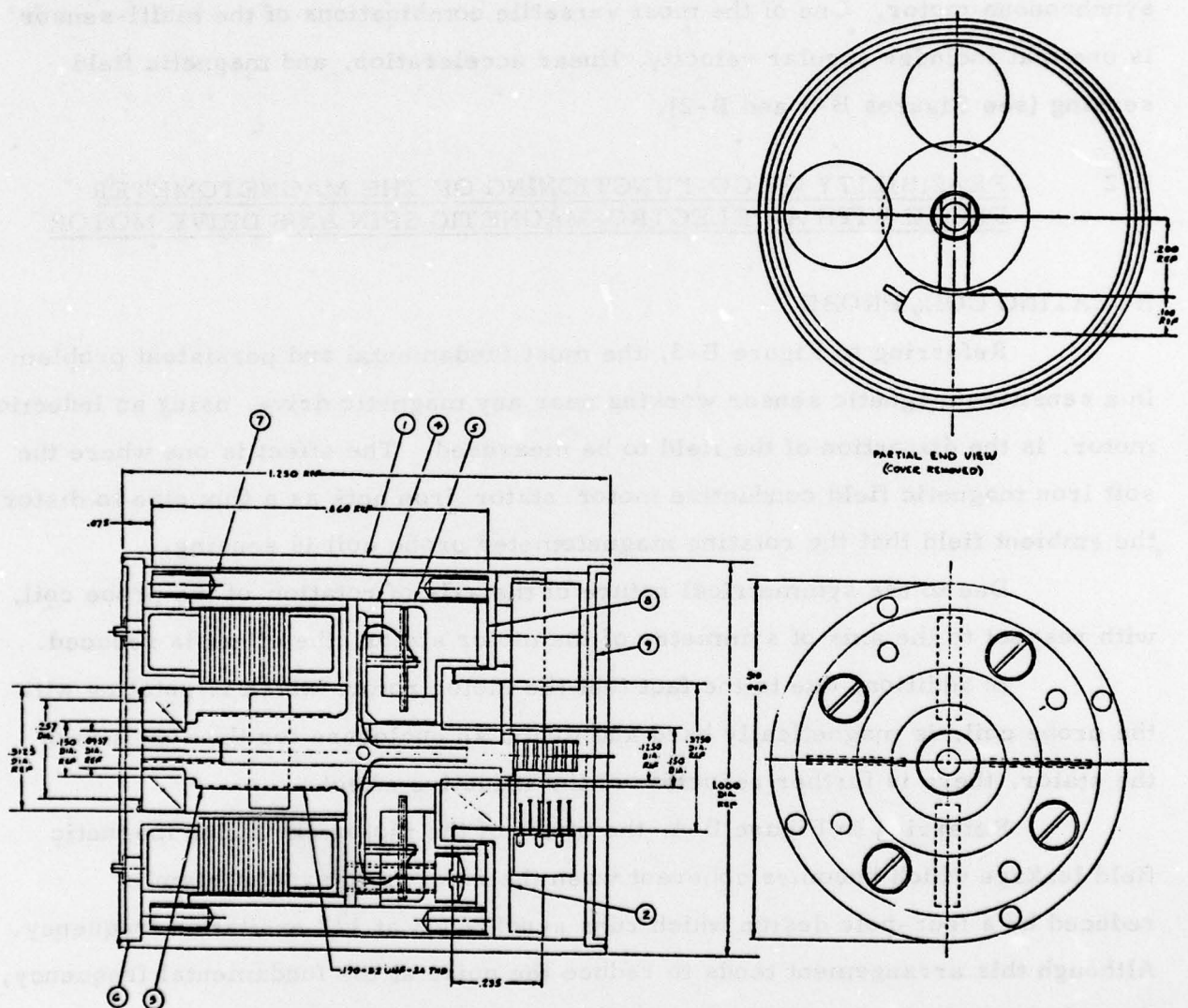


Figure B-1. Electrically Driven Multi-Sensor.

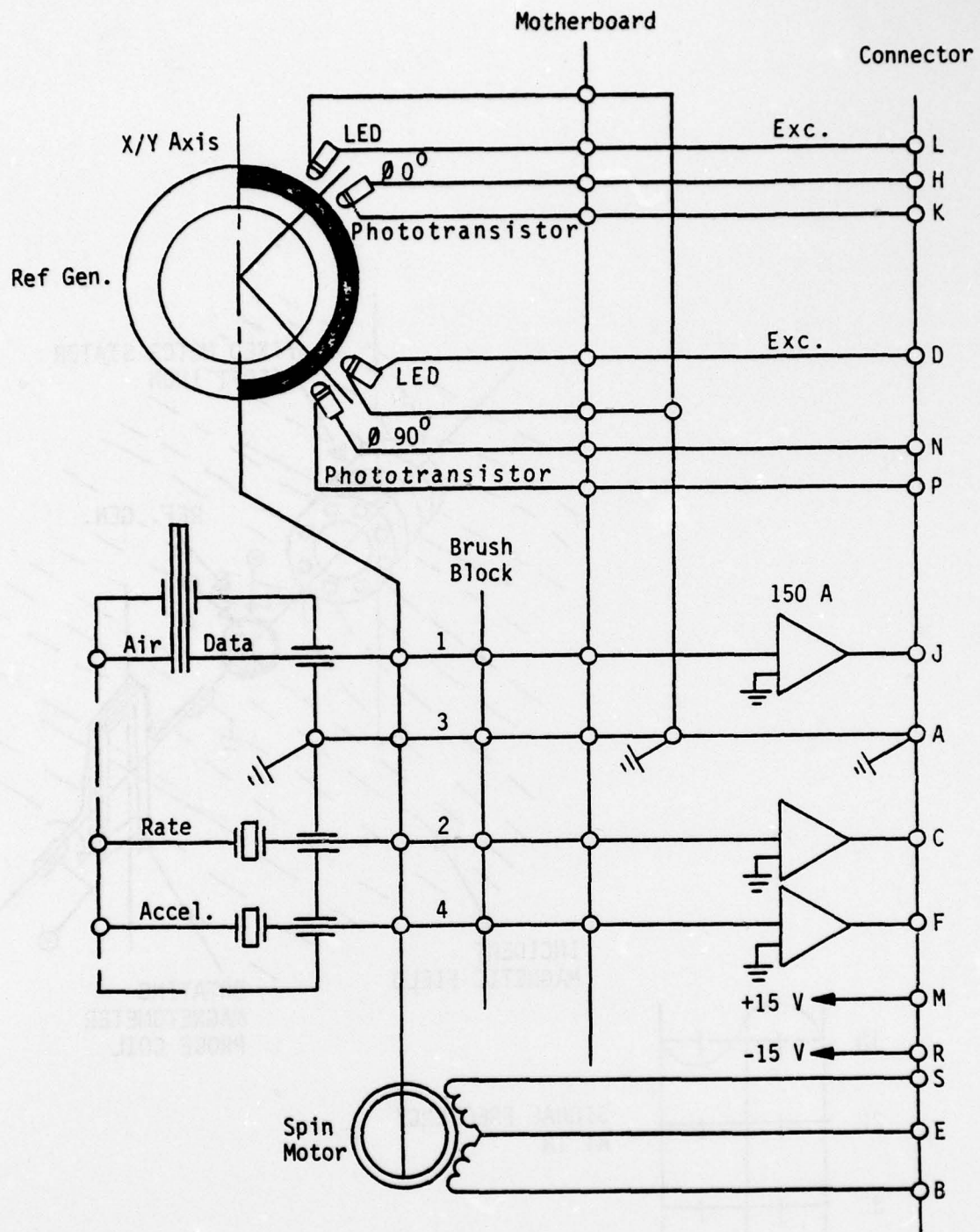


Figure B-2. Electrically Driven Multi-Sensor Schematic Diagram.

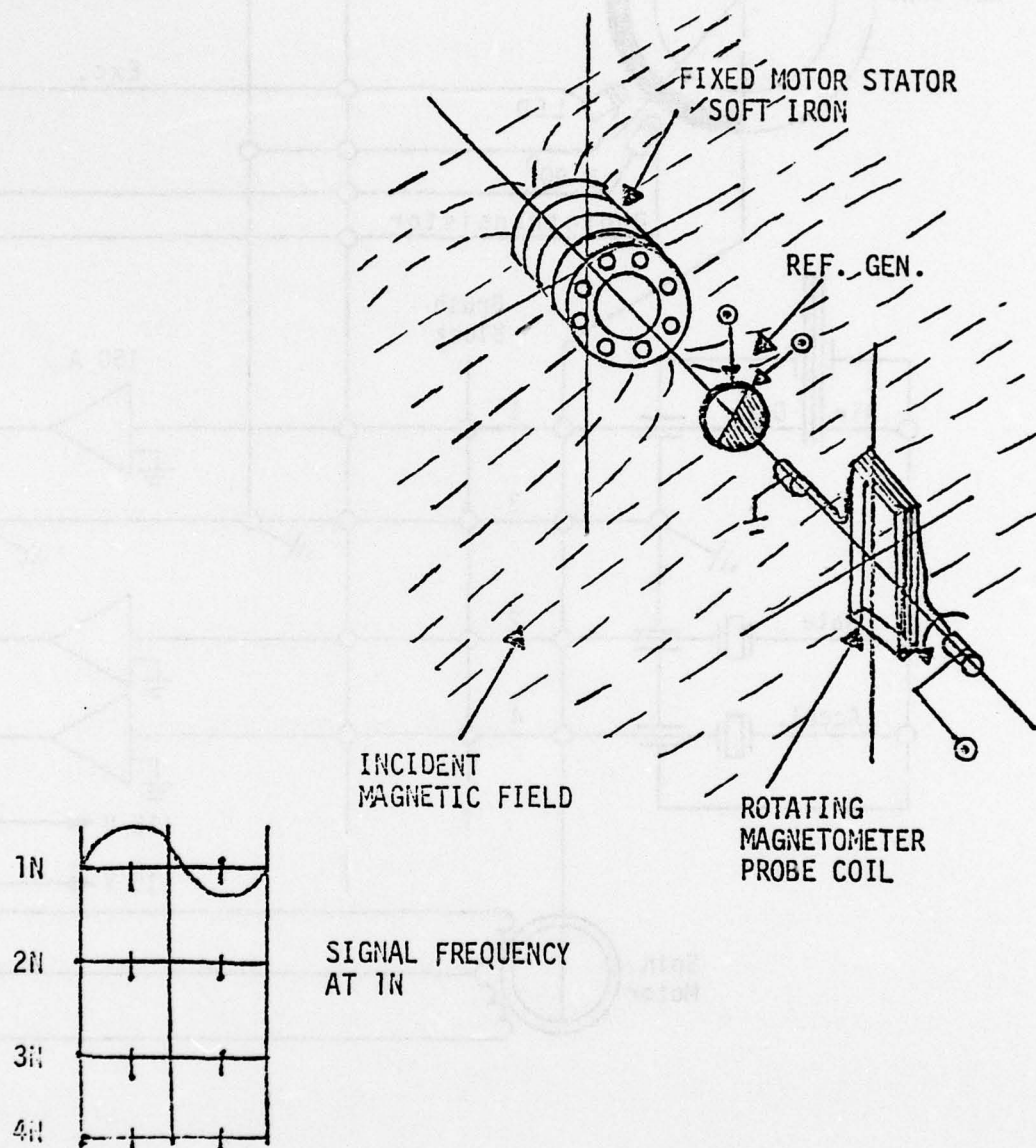
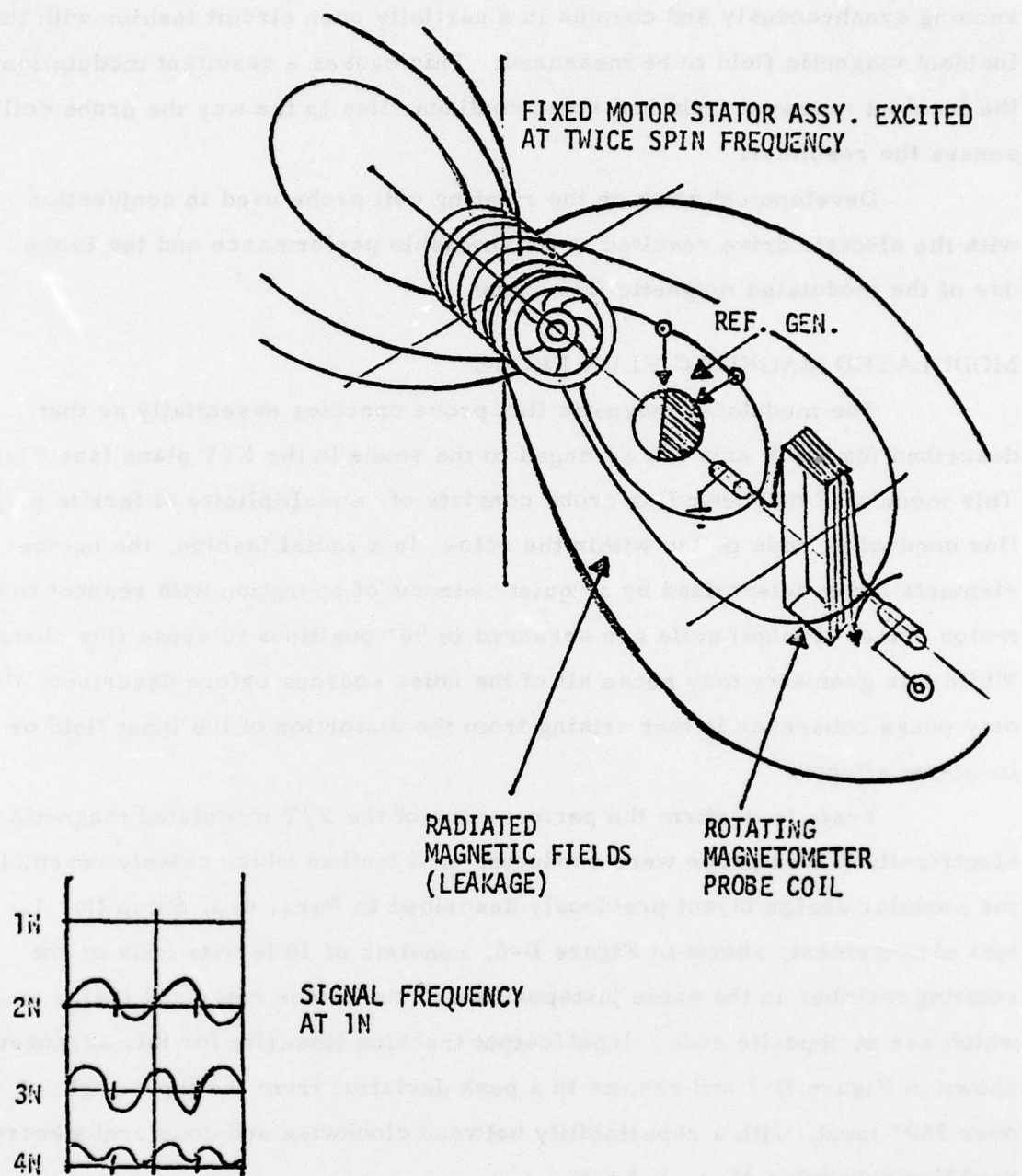


Figure B-3. Distortion of Field (Induction Effects).





**Figure B-4. Electro/Magnetic Spin Motor Noise Sources/Effects on Simple Coil Probe - Motor Excitation Losses.**

Referring to Figure B-5, one of the more subtle effects is that of the rotating magnetic dipole which is impressed into the motor rotor when it is running synchronously and couples in a partially open circuit fashion with the incident magnetic field to be measured. This causes a resultant modulation of the incident magnetic field and some nonlinearities in the way the probe coil senses the resultant.

Development work on the rotating coil probe used in conjunction with the electric drive resulted in unacceptable performance and led to the use of the modulated magnetic flux probe.

#### MODULATED MAGNETIC FLUX PROBE

The modulated magnetic flux probe operates essentially as that described for the Z axis but arranged to sense in the X/Y plane (see Figure B-6). This modulated magnetic flux probe consists of a multiplicity of ferrite magnetic flux conducting rods potted within the rotor, in a radial fashion, the number of elements being determined by a "quiet" window of operation with respect to the motor noise. Pickoff coils are arranged in 90° positions to sense flux change. While this geometry may sense all of the noise sources before described, the only phase coherence is that arising from the distortion of the input field or induction effects.

Tests to confirm the performance of the X/Y modulated magnetic flux electrically driven probe were conducted on a testbed which closely resembles the modular design layout previously described in Para. 4.2, Setup No. 3. This test arrangement, shown in Figure B-6, consists of 10 ferrite rods on the rotating member in the same juxtaposition to the motor rotor and stator assembly, which are at opposite ends. Input/output tracking linearity for this arrangement is shown in Figure B-7 and results in a peak deviation from the input angle of  $<.7^\circ$  over 360° input, with a repeatability between clockwise and counterclockwise tumbling schedules of  $<.3^\circ$  p-p.

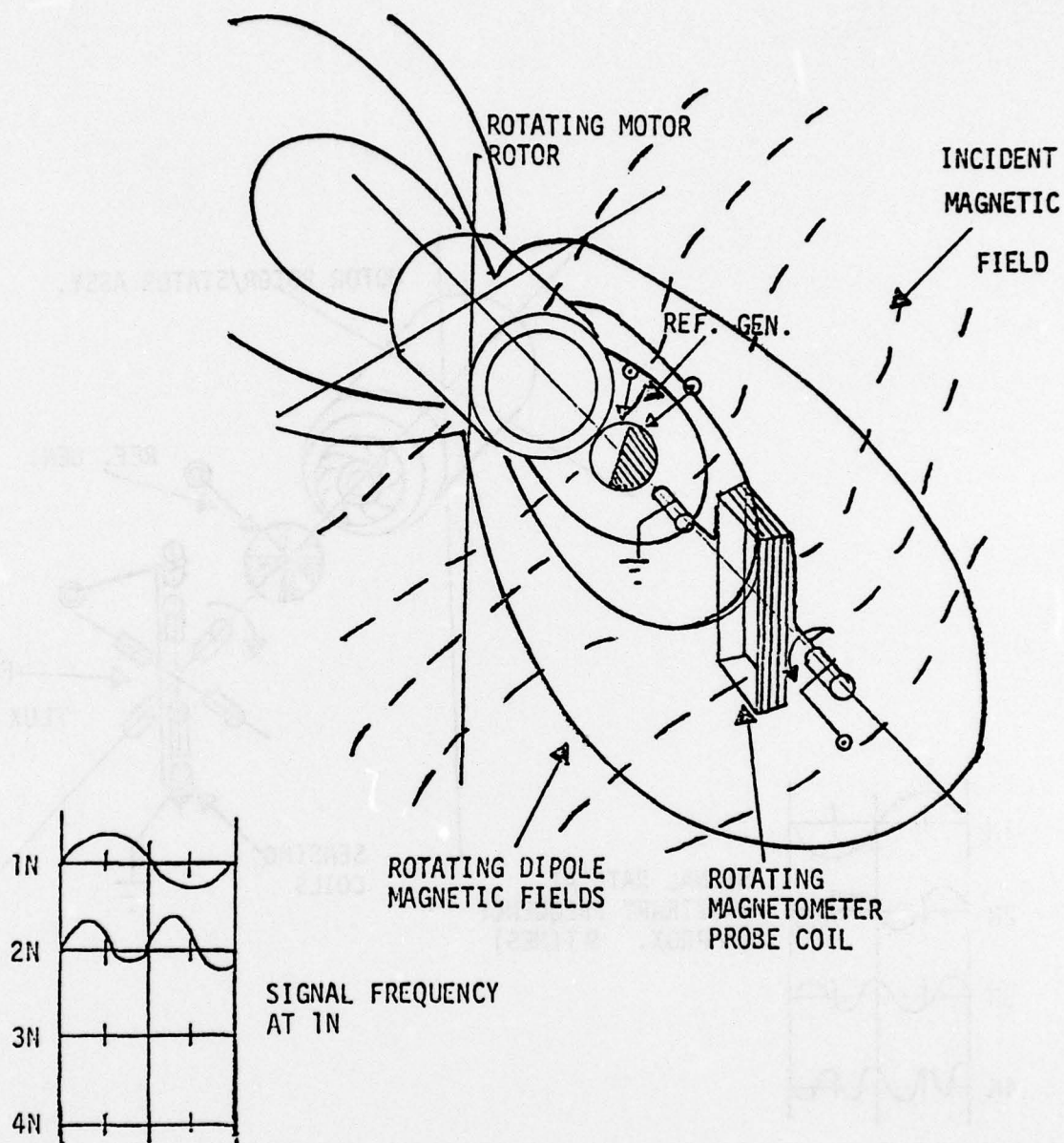


**Figure B-5. Electro/Magnetic Spin Motor Noise Sources/Effects on Simple Coil Probe - Inter-Field Reflective Effects**



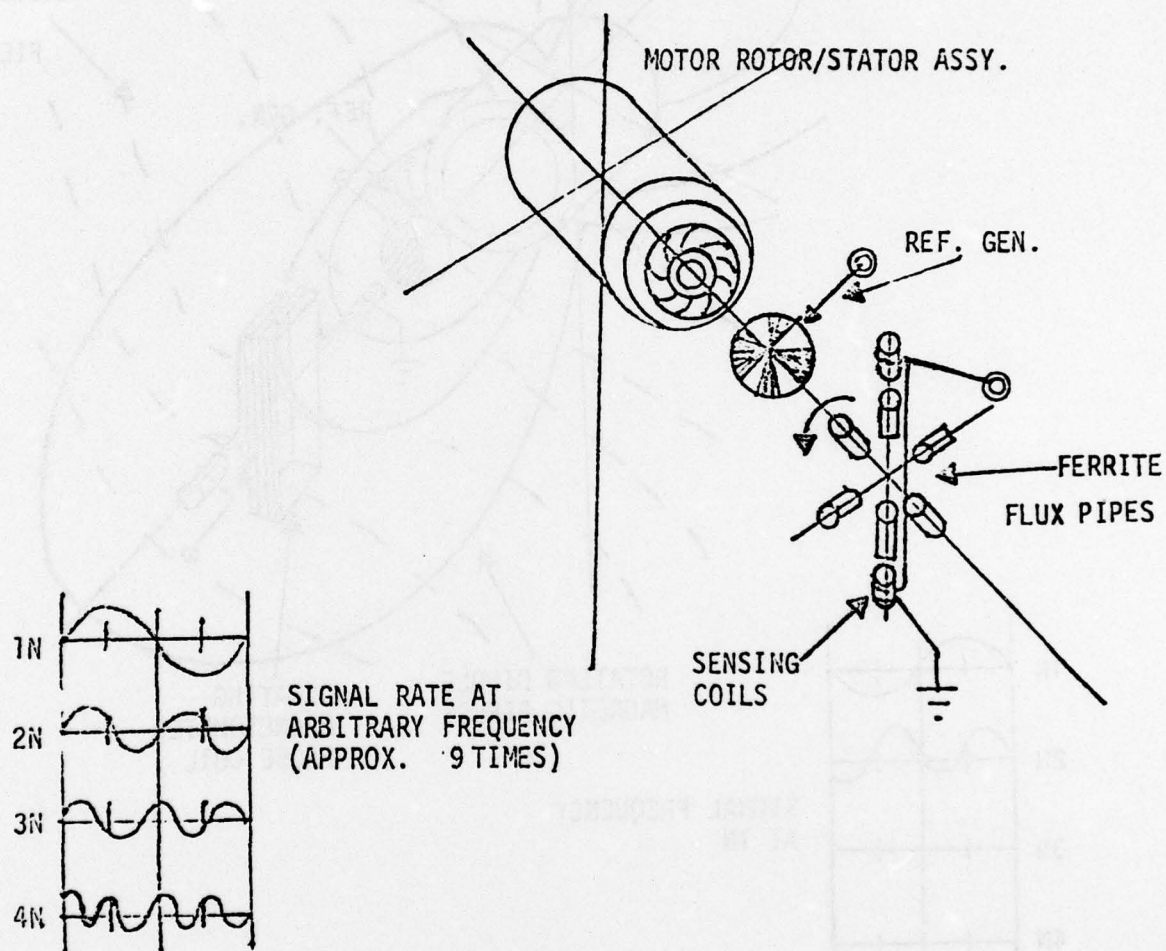


Figure B-6. Electro/Magnetic Spin Motor Noise Sources/Effects on Modulated Magnetic Flux Type Probe - X/Y Axis Configuration

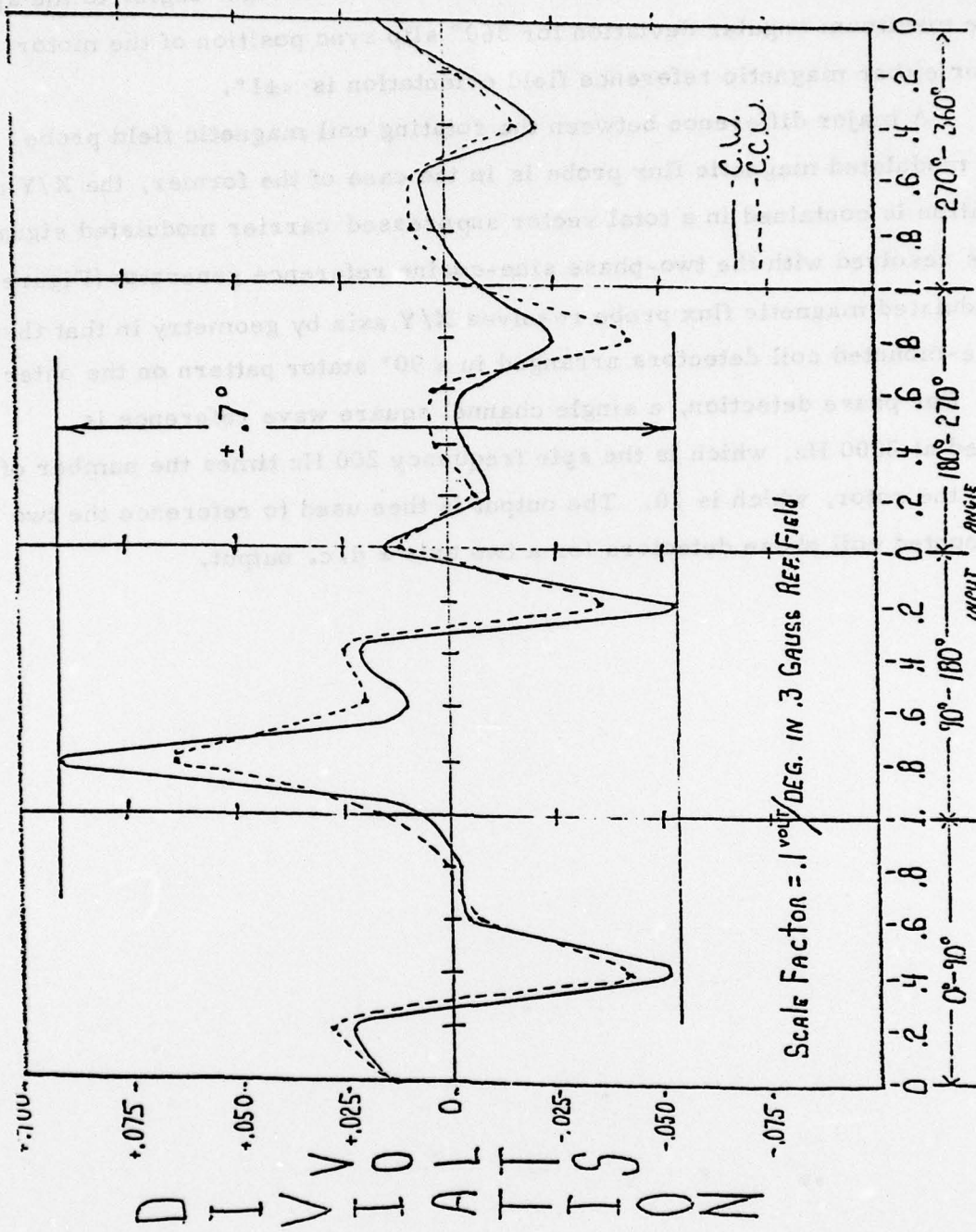


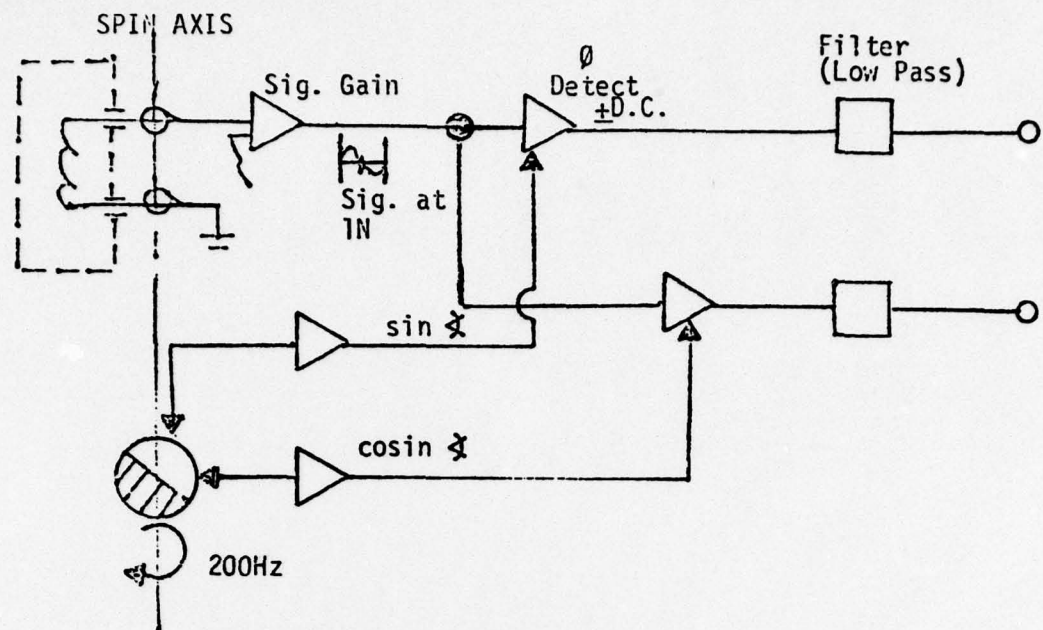
Figure B-7. Modulated Magnetic Flux Type Probe Test Bed  
(Tracking Accuracy).

If the motor rotor sync position is changed when the reference magnetic field is applied either along the spin axis or at right angles to the spin axis the maximum angular deviation for 360° slip sync position of the motor rotor for either magnetic reference field orientation is  $<\pm 1^\circ$ .

A major difference between the rotating coil magnetic field probe and the modulated magnetic flux probe is in the case of the former, the X/Y axis information is contained in a total vector suppressed carrier modulated signal which is resolved with the two-phase sine-cosine reference generator (Figure B-8). The modulated magnetic flux probe resolves X/Y axis by geometry in that there are case-mounted coil detectors arranged in a 90° stator pattern on the outer frame. For phase detection, a single channel square wave reference is generated at 2000 Hz, which is the spin frequency 200 Hz times the number of poles on the rotor, which is 10. The output is then used to reference the two case-mounted coil phase detectors for a two axis  $\pm$  d.c. output.



## I. ROTATING COIL PROBE



## II. MODULATED MAGNETIC FLUX PROBE

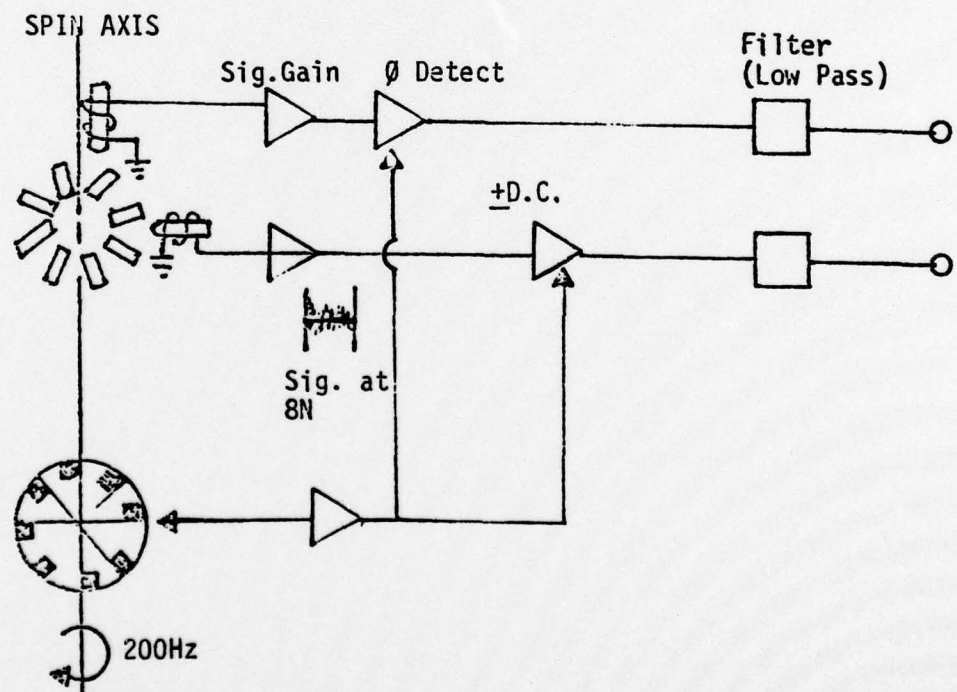


Figure B-8. Signal Detection.

## Appendix C

### GYRO STABILIZED ELECTRIC AND MAGNETIC FIELD EXPERIMENTAL SENSOR

One of the most important possible configurations for this multi-sensing technique is for a directly gyro stabilized electric and magnetic field sensor. The possibility for system performance improvement from such a sensor configuration is promising. An experimental magnetic and electric static force field sensing array was integrated into a conventional gas driven and erected vertical gyro. The primary object was to measure the expected improved performance of a gyro compass transmitter so configured. In addition, the electric sensor so stabilized by the gyro should give an additional degree of freedom for measuring the earth's atmospheric field free from vehicle dynamic motion.

The gyro stabilized electric and magnetic field sensor is shown schematically in Figure C-1, and, in addition to the primary measurement, includes means to sense the gravity direction with respect to the carrying vehicle.

The test sensor embodied the basic functional features of an air-driven and an air-erected vertical gyro with modifications necessary to include torquing the leveling system, signal transmission and gimbal angle transducing.

The gimbal angle transducing scheme, which is shown schematically in Figure C-2, consists of a simple radiating dipole arranged on the stable member coupling to pickoff coils arranged on the outer frame. The performance of this gimbal angle transducing scheme was evaluated and is shown in Table C-1.

The signal processor to operate this gyro stabilized electric and magnetic field sensor includes a display for the electric field sensed vertical and the gyro stabilized magnetic heading.

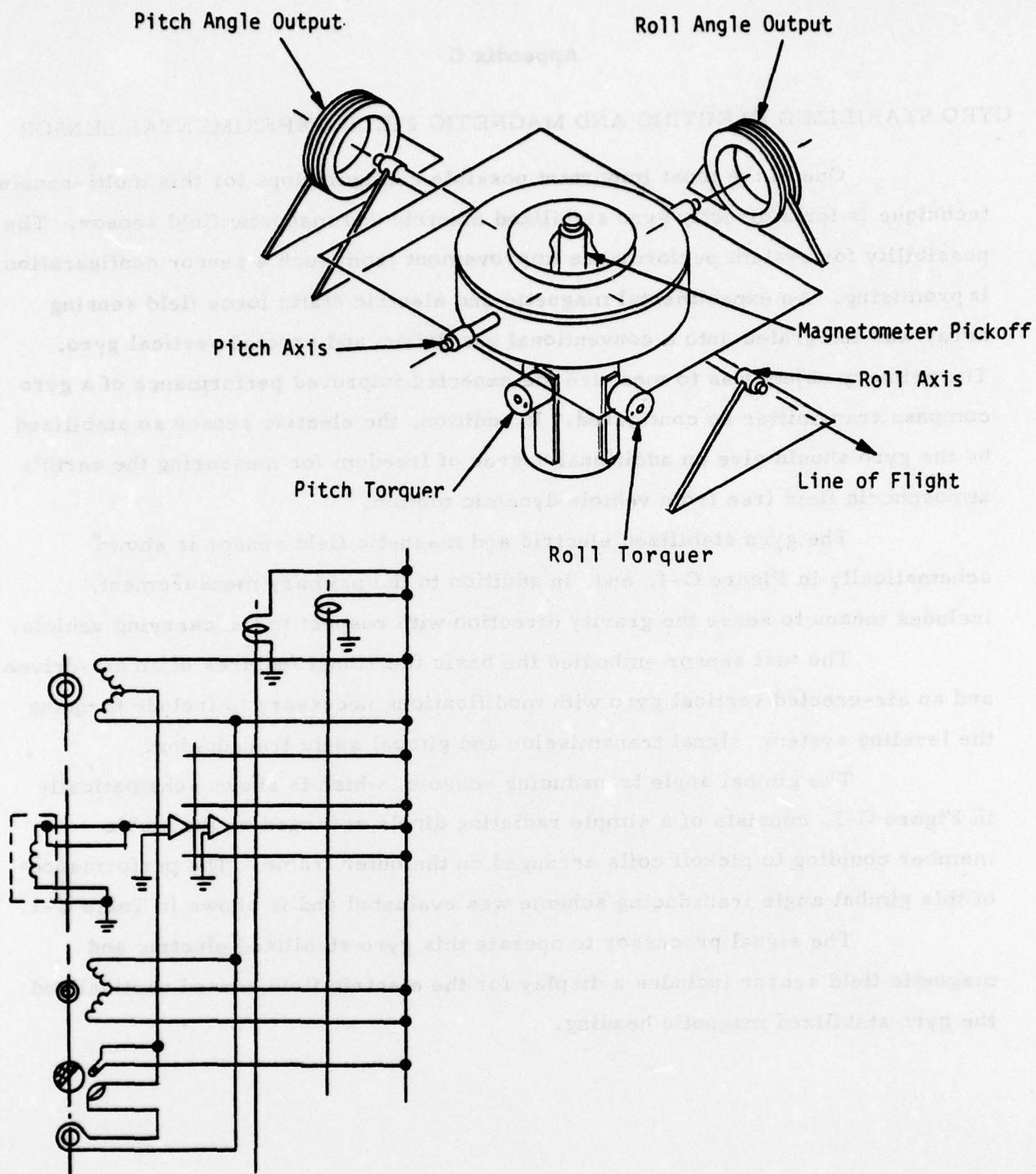


Figure C-1. Gyro Stabilized Electric and Magnetic Field Sensor.



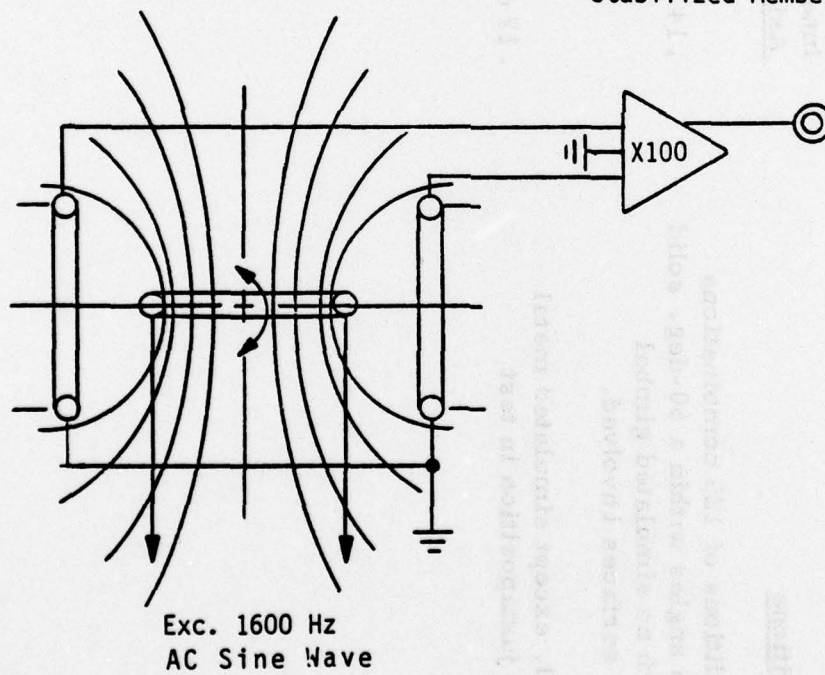
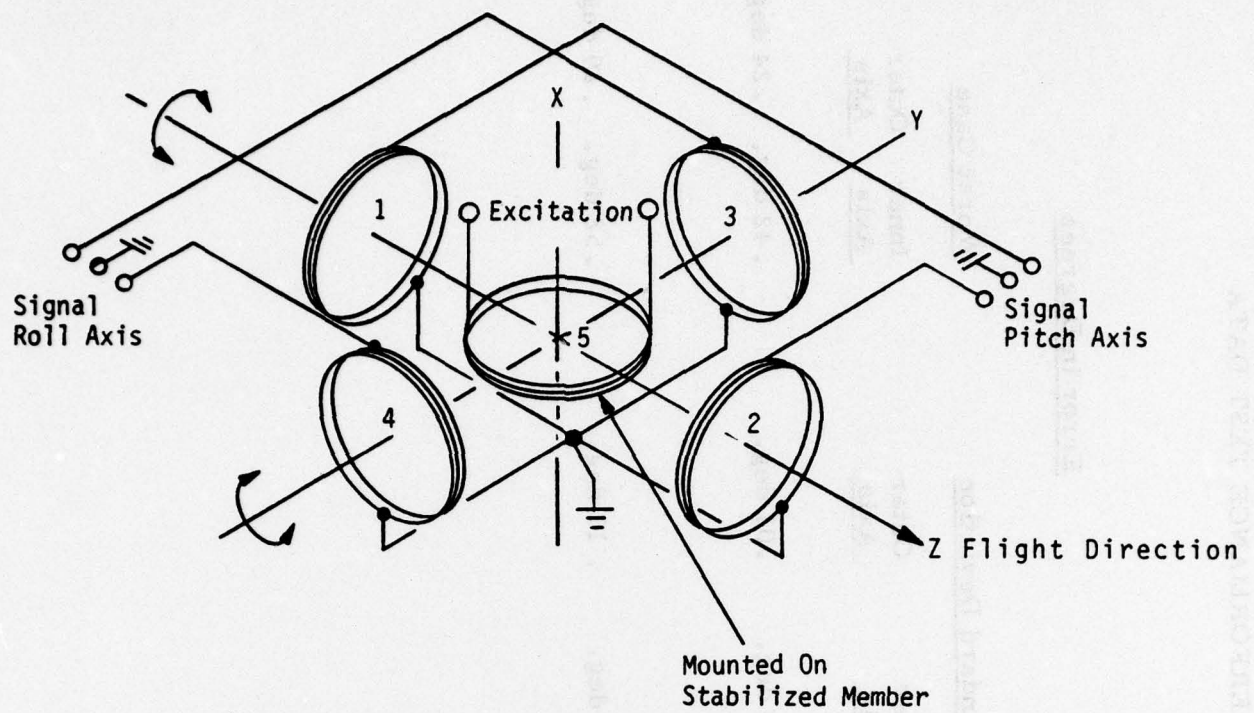


Figure C-2. Gimbal Angle Transducing Scheme.

TABLE C-1. GIMBAL PICKOFF PERFORMANCE TEST DATA

Test Conditions	<u>Error in Degrees</u>			
	<u>Standard Deviation</u>		<u>Worst Case</u>	
	<u>Inner Axis</u>	<u>Outer Axis</u>	<u>Inner Axis</u>	<u>Outer Axis</u>
1. Input conditions of 125 combinations of attitude angles within a 60-deg. solid angle, with no simulated gimbal reflective surfaces involved.	.14 deg.	.07 deg.	.42 deg.	.24 deg.
2. Same as 1, except simulated metal gimbal in juxtaposition in test setup.	.17 deg.	.11 deg.	.58 deg.	.29 deg.